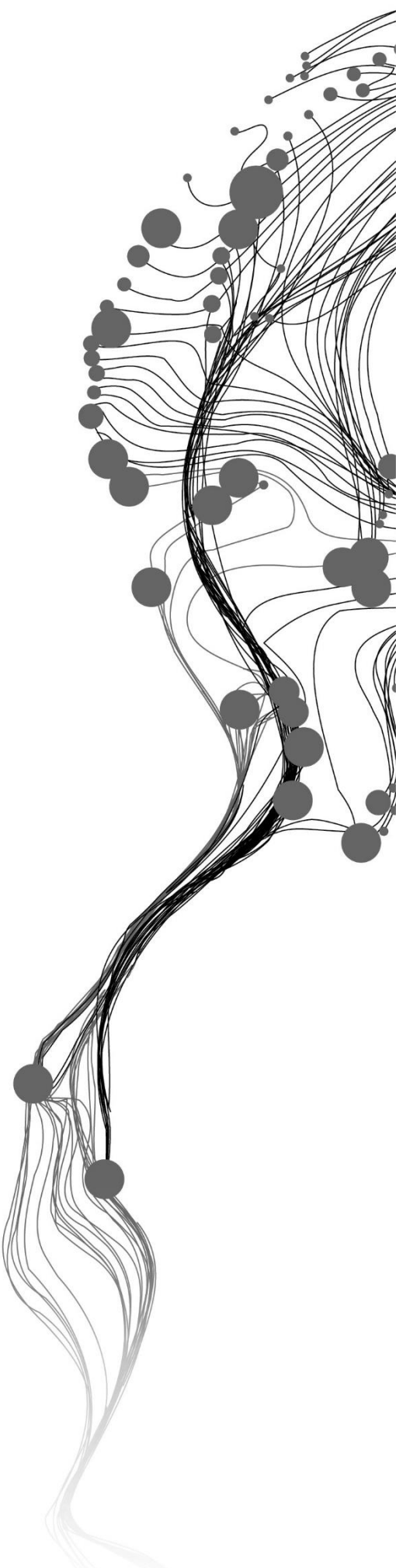


Quantifying root zone soil moisture at field scale through downscaling of SMAP Level 4 Soil Moisture product using Sentinel-1

URVI GAUTAM
February, 2018

SUPERVISORS:
Dr. Ir. Rogier van der Velde
Dr. Zoltan Vekerdy



Quantifying root zone soil moisture at field scale through downscaling of SMAP Level 4 Soil Moisture product using Sentinel-1

URVI GAUTAM

Enschede, The Netherlands, February, 2018

Thesis submitted to the Faculty of Geo-Information Science and Earth Observation of the University of Twente in partial fulfilment of the requirements for the degree of Master of Science in Geo-information Science and Earth Observation.

Specialization: Water Resources and Environmental Management (WREM)

SUPERVISORS:

Dr. Ir. Rogier van der Velde

Dr. Zoltan Vekerdy

Advisor: Ir. H.F. Benninga

THESIS ASSESSMENT BOARD:

Prof. Dr. Z. Su (Bob) (Chair)

Dr. D.C.M. Augustijn (External Examiner, University of Twente)

DISCLAIMER

This document describes work undertaken as part of a programme of study at the Faculty of Geo-Information Science and Earth Observation of the University of Twente. All views and opinions expressed therein remain the sole responsibility of the author, and do not necessarily represent those of the Faculty.

ABSTRACT

From past some years, microwave remote sensing with various frequencies has been widely used for soil moisture studies because of their ability to penetrate the clouds and monitor land surface under any atmospheric conditions. Remote sensing is an effective technique for estimating soil moisture at various spatial scales. NASA's Soil Moisture Active Passive (SMAP) Level 4 soil moisture products are the value-added model-derived soil moisture product for which the SMAP Level 1 brightness temperatures are assimilated in to the GEOS-5 catchment land surface model. The available SMAP L4_SM products are at a coarse resolution of 9 km that cannot be used in field scale such as agricultural applications. So, to use this data in a field scale, it is required to downscale these product to a spatial resolution that will be relevant for agricultural applications. The main purpose of this study is to downscale the available SMAP surface and root zone soil moisture estimates to check it's applicability in field scale.

Many studies have supported that the fusion of radar data and radiometer soil moisture data has a high potential to get soil moisture at fine resolution. A similar approach is followed in this study, SMAP L4 soil moisture products have been combined with fine resolution Sentinel-1 SAR data. First an exponential relationship between surface and root zone soil moisture indices obtained from SMAP L4 data has been developed. Then the backscattering data obtained from Sentinel-SAR has also been linearly related to surface soil moisture index. The most optimum soil sensitive parameters were selected for each SMAP pixel considering for VV and VH backscattering separately. These parameters were used in the baseline algorithm to downscale surface soil moisture. The downscaled surface soil moisture were used to downscale root zone soil moisture using the relationship obtained initially. Thus, surface and root zone soil moisture product for VV and VH polarization were obtained.

The soil moisture product before and after downscaling were validated against the in-situ measurement obtained from the 20 soil moisture measurement stations in the Twente region placed by the Faculty of Geo-information Science and Earth Observation (ITC) of the University of Twente. It was found that the downscaled surface soil moisture from VV showed a better result than VH. The downscaled surface soil moisture from VV showed the RMSE of $0.062 \text{ m}^3\text{m}^{-3}$ and R^2 of 0.593 which is better than the original product which had RMSE $0.066 \text{ m}^3\text{m}^{-3}$ and R^2 0.573. However, in case of root zone soil moisture the validation results were not satisfying. Although the downscaled root zone soil moisture from VV showed a better result than VH, it was still not able to maintain the accuracy of the original SMAP L4 product and showed some degradation after downscaling with R^2 decreasing from 0.36 to 0.266. This can be mainly attributed to the underlying model parameters and the limited number of soil moisture monitoring stations available for validation of root zone soil moisture. Overall it can be said that the proposed method is applicable for downscaling SMAP surface soil moisture which increased the accuracy of original product and gave a result with better spatial resolution and land surface details relevant for agricultural application. Whereas, downscaling of SMAP root zone soil moisture is difficult with this approach because of the embedded model parameters.

Keywords: SMAP L4 surface soil moisture, SMAP L4 root zone soil moisture, Sentiel-1 SAR Backscattering coefficient, in-situ soil moisture measurements, Downscaling

ACKNOWLEDGEMENTS

First and foremost, I would like to express my sincere gratitude to my supervisors, Dr. Ir. R. Van der Velde and Dr. Z. Vekerdy for their valuable suggestions, feedbacks and proper guidance. This thesis would not have been completed without their support. I would also like to thank my advisor Ir. H.F. Benninga (PhD student) for helping me through my work.

I would like to thank Netherland Fellowship Programme (NFP) for providing this opportunity to pursue my MSc degree at ITC.

I would also like to thank my family, back home for their immense support, encouragement and belief in me whenever I was feeling low. I am thankful to my friends for always motivating me. And finally I would like to thank Enschede Nepali Family for providing me an environment of home away from home during my stay in Enschede.

LIST OF ABBREVIATIONS

ALOS	Advanced Land Observing Satellite
AMSR-E	Advanced Microwave Scanning Radiometer for EOS
ASCAT	Advanced SCATterometer
BOFEK	BOdemFysische EenhendenKaart
BRP	Basic Registration of crop Parcel
GEOS-5	Goddard Earth Observation Model System, Version-5
GRD	Ground Range Detected
IW	Interferometric Wide
L4	Level-4
NASA	National Aeronautics and Space Administration
NSIDC	National Snow and Ice Data Centre
OSSE	Observation System Simulation Experiment
PALSAR	Phased Array L-band SAR
PALS	Passive and Active L-band and S-band
RMSE	Root Mean Square Error
RSMI	Root zone Soil Moisture Index
SAR	Synthetic Aperture Radar
SM	Soil Moisture
SMAP	Soil Moisture Active Passive
SMEX02	Soil Moisture Experiment 2002
SMI	Soil Moisture Index
SMOS	Soil Moisture Ocean and Salinity
SNAP	Sentinel Application Platform
SSMI	Surface Soil Moisture Index
VH	Vertical transmit and Horizontal receive
VV	Vertical transmit and Vertical receive
WUR	Wageningen University and Research

TABLE OF CONTENTS

List of figures.....	viii
List of tables.....	x
1. Introduction.....	1
1.1. Scientific background.....	1
1.2. Research Problem.....	3
1.3. Objectives.....	4
1.4. Research Questions.....	4
1.5. Thesis Structure.....	4
2. Study area and data sets.....	5
2.1. Twente region.....	5
2.2. Datasets.....	6
2.2.1. Land Cover data.....	6
2.2.2. Soil Properties data.....	6
2.2.3. In-situ measurement data.....	7
3. Satellite products.....	10
3.1. SMAP L4_SM product.....	10
3.2. Sentinel-1 SAR.....	11
4. Research Methodology.....	13
4.1. Methodology Flowchart.....	13
4.2. Translating SMAP L4 Soil moisture into Soil Moisture Index.....	14
4.3. Downscale surface soil moisture index.....	14
4.4. Downscale root zone soil moisture index.....	15
4.5. Errors metrics.....	16
5. Development of relationships.....	17
5.1. Sentinel- 1 SAR backscatter vs SMAP L4 SSMI.....	17
5.2. SMAP L4 SSMI vs RSMI.....	22
6. Validation.....	24
6.1. SMAP L4 surface soil moisture product.....	24
6.2. SMAP L4 root zone soil moisture product.....	26
6.3. Downscaled surface soil moisture.....	27
6.4. Downscaled root zone soil moisture.....	30
7. Downscaling results.....	33
7.1. Downscaled surface soil moisture.....	33
7.2. Downscaled root zone soil moisture.....	35
8. Discussion.....	37
9. Final remarks.....	40
9.1. Conclusions.....	40
9.2. Limitations and Recommendations.....	41
List of references.....	42
Appendices.....	46

LIST OF FIGURES

Figure 1: Location of Twente inside the Netherlands and map of the Twente region	5
Figure 2: The dynamics of rainfall pattern in Twente region for the year 2016.	5
Figure 3: Land cover map of 2016 showing the different land cover classes of the Twente region.....	6
Figure 4: The soil unit properties map for Netherlands obtained from BOFEK2012.	7
Figure 5: Google earth image showing the study area of Twente and red dots shows the distribution of the 20 soil moisture measurement stations placed by the ITC in twente region.	8
Figure 6: (a) is sample of soil moisture monitoring station in the study area and (b) shows the data recorded by this station being downloaded.	9
Figure 7: SMAP L4 image of 1st January 2016 in the study area of the Twente region which gives the estimates of soil moisture content in each pixel.	11
Figure 8: A sample image of Sentinel-1 SAR showing the region of Twente and acquired on 7 th January 2016 after the completion of pre-processing steps.	12
Figure 9: A schematic representation of the procedures involved in combining SMAP L4_SM product and Sentinel-1 SAR data to retrieve downscaled surface and root zone soil moisture product.	13
Figure 10: SMAP SSMI plotted against backscattering coefficient ($\sigma^{o_{VH}}$ and $\sigma^{o_{VV}}$) for selected pixel (7,1)..	17
Figure 11: SMAP SSMI plotted against the normalized backscattering coefficient ($\sigma^{o_{VH_ref}}$ and $\sigma^{o_{VV_ref}}$) for the selected pixel (7,1).	19
Figure 12: Figure showing the correlation between surface soil moisture index and backscattering coefficient for selected pixel for different orbital passes.....	20
Figure 13: Scatter plot showing the agreement between SMAP surface and root zone soil moisture index, scatter plot for pixel (0,0) shows the highest and scatter plot for pixel (2,2) shows the lowest out of 24 pixels.	23
Figure 14: Time series showing the average retrieved coarse resolution SMAP surface soil moisture against the averaged in-situ soil moisture measurements for the study area and the rainfall data.	24
Figure 15: Time series showing the averaged retrieved coarse resolution SMAP surface soil moisture against the averaged in-situ soil moisture measurements and the rainfall data after the bias correction of SMAP data.	25
Figure 16: Time series showing the averaged retrieved coarse resolution SMAP root zone soil moisture against the averaged in-situ soil moisture measurements and the rainfall data after the bias correction of SMAP data.	27
Figure 17: Time series showing the averaged retrieved downscaled SMAP surface soil moisture for $\sigma^{o_{VH}}$ against the averaged in-situ soil moisture measurements and the rainfall data after the bias correction of SMAP data.	28
Figure 18: Time series showing the averaged retrieved downscaled SMAP surface soil moisture for $\sigma^{o_{VV}}$ against the averaged in-situ soil moisture measurements and the rainfall data after the bias correction of SMAP data.	29
Figure 19: Time series showing the averaged downscaled SMAP root zone soil moisture for $\sigma^{o_{VH}}$ against the averaged in-situ soil moisture measurements and the rainfall data after the bias correction of SMAP data.	31
Figure 20: Time series showing the averaged downscaled SMAP root zone soil moisture for $\sigma^{o_{VV}}$ against the averaged in-situ soil moisture measurements and the rainfall data after the bias correction of SMAP data.	31
Figure 21: Series of surface soil moisture map downscaled to a resolution of 50 m obtained from combining SMAP L4 surface soil moisture and Sentinel-1 SAR backscattering coefficient.	34
Figure 22: Series of root zone soil moisture map downscaled to a resolution of 50 m obtained from the relationship deduced between SMAP L4 surface and root zone soil moisture product.	36

Figure 23: A time series showing the response of σ_{VH} , σ_{VV} and $\sigma_{VH} - \sigma_{VV}$ for different land cover types (Grassland, Corn field and Forest)..... 38

Figure 24: Scatter plot where (a) and (b) shows the agreements between SMAP surface soil moisture and in-situ measurements for summer and winter seasons and (c) and (d) shows the agreements between downscaled SMAP surface soil moisture and in-situ measurements..... 39

LIST OF TABLES

Table 1: Characteristics of high resolution Level-1 IW Sentinel-1 (Sentinel 1 Team, 2013).....	11
Table 2: The parameters ($\alpha_{(C)}$ and $\beta_{(C)}$) for equation (3) and R^2 obtained from the linear relationship between aggregated $\sigma^{\circ_{VH}}$ and SMAP SSMI for all the 24 pixels in the study area. The bold values show the minimum and the maximum range of R^2	17
Table 3: The parameters ($\alpha_{(C)}$ and $\beta_{(C)}$) for equation (3) and R^2 obtained from the linear relationship between $\sigma^{\circ_{VV}}$ and SMAP SSMI for all the 24 pixels in the study area. The bold values show the minimum and the maximum range of R^2	18
Table 4: Soil moisture sensitive parameters ($\alpha_{(C)}$ and $\beta_{(C)}$) and R^2 for all 24 pixels and 4 orbital passes for $\sigma^{\circ_{VH}}$. The bold values show the minimum and the maximum range of $\beta_{(C)}$ and R^2	21
Table 5: Soil moisture sensitive parameters ($\alpha_{(C)}$ and $\beta_{(C)}$) and R^2 for all 24 pixels and 4 orbital passes for $\sigma^{\circ_{VV}}$. The bold values show the minimum and the maximum range of $\beta_{(C)}$ and R^2	21
Table 6: The parameters (a and b) from equation (9) and R^2 obtained from the relationship developed between the SMAP SSMI and RSMI for all 24 pixels. The bold values show the minimum and the maximum range.....	23
Table 7: Error metrics (ubRMSE and R^2) for surface soil moisture retrieved from each SMAP pixel and the corresponding soil moisture monitoring stations in it. The bold values show the minimum and the maximum range.....	25
Table 8: Error metrics (ubRMSE and R^2) for root zone soil moisture retrieved from each SMAP pixel and the corresponding field measurement stations in it. The bold values show the minimum and the maximum range.....	27
Table 9: Error metrics (ubRMSE and R^2) for individual field measurement stations and its corresponding downscaled surface soil moisture data for $\sigma^{\circ_{VH}}$ averaged to 5×5 grid cells around the stations.....	29
Table 10: Error metrics for weighted average of field measurements from individual station and its corresponding downscaled surface soil moisture data for $\sigma^{\circ_{VH}}$ and $\sigma^{\circ_{VV}}$ which is the averaged data of 5×5 grid cells around the stations.....	32

1. INTRODUCTION

1.1. Scientific background

Soil moisture is an important land state variable that governs water and energy exchanges between the atmosphere and land surface (Das et al., 2011). Soil moisture acts as a controlling variable by partitioning rainfall into recharge, runoff and evapotranspiration. (Pierdicca et al., 2013) and plays an important role in various applications such as flood forecasting, regional water management, agriculture, etc. The water available in the soil which can be taken up by the vegetation for its development is considered as the natural source of water for crops and is one of the determining factors for increasing or decreasing crop productivity (Pitts, 2016). In agriculture, the efficient irrigation scheduling and an improved crop yield forecasting can be achieved if a proper moisture conditions in the root zone is maintained (Giacomelli et al., 1995). The root of the plants can outspread from few centimetres below the soil surface up to two meters depending upon the types of crops (Baldwin et al., 2017). In this study the root zone depth is considered up to 1 m assuming that the most part of the root is present within this depth range (Jackson et al., 1996).

Reliable soil moisture estimation is important to develop plans and strategies for skilful crop water management. There are different field measurement techniques and satellite observations, which can provide the soil moisture estimates. Although in-situ measurements are considered to be accurate, they are point measurements and are always limited to a small scale and scarce across larger domains. In-situ soil moisture measurements are relatively expensive and often time consuming to collect (Houser et al., 1998). It is also difficult to measure soil moisture representative in field for large areas because of its temporal and spatial variability. In contrast to the field measurement methods, remote sensing is an effective technique for estimating soil moisture across various spatial scales (Taktikou et al., 2016). Over the past decades, microwave remote sensing with various frequencies (X, C and L bands) has been widely used for soil moisture studies mainly because of their sensitivity for the soil moisture content and vegetation water content (Calvet et al., 2011). Microwave remote sensing is mostly preferred for soil moisture studies because of their ability to penetrate the clouds and monitor land surface under any atmospheric conditions (Njoku & Entekhabi, 1996).

The C and X band microwave sensors like Advanced Microwave Scanning Radiometer, AMSR-E (Radiometer with 6 bands, V and H polarization, 6.9 to 89 GHz) and Advanced SCATterometer, ASCAT (C-band scatterometer, VV polarization 5.255 GHz) provides the global surface wetness measurements (Brocca et al., 2011) but are more relevant for the area with less vegetation as they are more sensitive towards vegetation water content. Whereas, the L-band sensors like Soil Moisture and Ocean Salinity, SMOS (1.4 GHz) and Soil Moisture Active Passive, SMAP (1.41 GHz (passive), 1.26 GHz (active)) provides near-surface soil moisture measurements and are found to be more sensitive towards soil moisture (Mohanty et al., 2017). These L-band sensors provide soil moisture data at a global scale and are also relevant for densely vegetated conditions. These datasets are in public domain and can be acquired.

On 31st January, 2015 NASA's Soil Moisture Active Passive (SMAP) mission was launched with an objective of global soil moisture and landscape freeze/thaw state mapping (Colliander et al., 2017). SMAP generates 15 distributable data products representing four levels of processing where Level 1 products are the instrument observed data. Level 2 data are the geophysical retrievals of soil moisture based on Level 1 data, Level 3 products are the daily composites of Level 2 soil moisture product and Level 4 are the value-

added model-derived soil moisture product for which the SMAP Level 1 brightness temperatures are assimilated into a land surface process model (NASA, 2014). The soil moisture product that uses the direct instrument measurements gives the volumetric soil moisture content for the top 5 cm of the soil column and does not include root zone information. These soil moisture estimates are available at a spatial resolution of 36 km and are not able to represent the spatial distribution of soil moisture for a heterogeneous land surface which restricts its use for agricultural applications (Entekhabi et al., 2008).

Many hydrological and agricultural applications like flood forecasting and drought monitoring require root zone soil moisture measurements (Schneider et al., 2014), which is not directly measured by microwave remote sensing. Thus, to reduce this gap the SMAP team has produced a level 4 soil moisture (L4_SM) product, which gives estimates of surface and root zone soil moisture. These products are the result of assimilation of SMAP level 1 brightness temperature into the Goddard Earth Observing System (GEOS-5) catchment land surface model (Reichle et al., 2016). These estimates have an improved spatial and temporal resolution over the original SMAP observations with a 9 km spatial resolution and 3-hourly temporal resolution (NASA, 2014).

The available SMAP L4_SM products are at a coarse resolution of 9 km that cannot be used for agricultural applications, such as irrigation management and estimation of plant productivity. A solution for using this data at a field scale is by downscaling these products to a spatial resolution which would give a better representation of the land surface heterogeneity in the field which will be relevant for agricultural applications. Many previous studies (e.g., Song et al., 2014; Njoku et al., 2002) have suggested to use radiometer soil moisture product with the fine resolution radar data to obtain soil moisture at a finer resolution. Njoku et al., (2002) developed a change detection algorithm based on the near linear relationship between the surface soil moisture data and backscatter data in a sparse vegetated condition assuming it to be homogeneous. The data acquired by Passive and Active L-band and S-band airborne sensor (PALS) during the Southern Great Plains Experiments in 1999 (SGP99) were used for the development of this algorithm. This change detection algorithm was also used by Narayan et al., (2006) to retrieve high resolution soil moisture data. Piles et al., (2009) used the change detection approach with the data obtained from PALS and Observation System Simulation Experiment (OSSE) and were able to set a result with a better identification of the error sources.

The change detection algorithm was further used and modified by Das et al., (2011) and was proposed as the SMAP baseline algorithm which was proved to be a simple yet robust approach to combine radar and radiometer data for retrieving absolute soil moisture estimates at fine resolution. In this algorithm Das et al., (2011) used a linear relationship between the time series information of radar and radiometer data unlike the earlier change detection method where previous satellite overpass was required. The robustness of the SMAP baseline algorithm was tested by Das et al., (2014) and the active/passive algorithm was proposed to be comparatively better than the previous soil moisture disaggregating algorithm. These past studies mainly focused on downscaling surface soil moisture as remote sensing data could only give the reading for top 5 cm of the soil surface. Since the main idea of this study is to downscale root zone soil moisture, an additional analysis is required regarding the retrieval of fine resolution root zone soil moisture so that it can be relevant for agricultural applications.

Estimation of root zone soil moisture has always been a challenge for researchers as it has a nonlinear relationship with surface soil moisture and vary a lot in time and in space (Dumedah et al., 2015). Many studies in the past have been done (e.g., Das et al., 2008; Dumedah et al., 2015) where they have used remotely sensed soil moisture data in various land surface models and have tried to quantify root zone soil moisture at a small scale. However, the SMAP L4_SM data used in this study are already an assimilated data obtained from the catchment model of Koster et al., (2000). So, a statistical relationship between SMAP L4

surface and root zone soil moisture is developed. This relationship is further used with downscaled surface soil moisture to get root zone soil moisture estimation at finer resolution.

The downscaling of SMAP L4 surface soil moisture is done using the baseline algorithm for which the main input is the backscatter data obtained from Sentinel-1 SAR. Baseline algorithm uses the approach of combining high resolution radar data with low resolution radiometer observation to retrieve a medium resolution product which possess the advantage to both radar resolution and radiometer sensitivity. In general the fusion of radar data and radiometer soil moisture data has a high potential to get soil moisture at fine resolution (Peng et al., 2017) but the main limiting factor for the use of fine resolution radar images is the lack of frequent acquisition of the images. For instance ALOS PALSAR images have the revisit time of 12 days in average which makes it difficult to analyse the time series of soil moisture. Sentinel-1 SAR on the other hand shows a better spatial resolution of 10 m and temporal resolution of every 3-6 days giving a comparatively sufficient data for combining with the available SMAP L4_SM product which is available for every 3 hours.

Sentinel-1 SAR data has been demonstrated to be sensitive to the soil moisture content and the C-band wavelength of SAR is marginally affected by changes in atmospheric composition (Yue et al., 2016). Along with better temporal resolution Sentinel-1 SAR image also have dual polarization (VV and VH) which can help in distinguishing certain land surface features as each polarization have different sensitivities to different surface types (Paloscia et al., 2013) but the backscattering coefficient provided by SAR is influenced by various factors like surface roughness and vegetation cover (Korres et al., 2013). However, combining radar data with radiometer soil moisture product will compensate to some extent, the errors due to radar sensitivity and radiometer resolution. Previous studies done over downscaling soil moisture mainly focused on surface soil moisture but in this study surface soil moisture (5 cm) is downscaled to a finer resolution which is further used to downscale root zone (top 1 m) soil moisture and is done by combining SMAP L4 soil moisture product with Sentinel-1 SAR data.

1.2. Research Problem

The available SMAP L4_SM product gives the estimates for both surface and root zone soil moisture at a spatial resolution of 9 km and temporal resolution of 3 hours. In a study done by Reichle et al. (2016), the SMAP L4_SM product when validated against in-situ measurements showed the uncertainty value of below $0.04 \text{ m}^3 \text{ m}^{-3}$ for both surface and root zone soil moisture which is considered as the required acceptable accuracy value for soil moisture product like SMAP (Entekhabi et al., 2010; Kerr et al., 2010). In spite of being a reliable product, it is still difficult to use these data for agricultural applications because of the rather coarse spatial resolution of 9 km which is not capable of representing soil moisture spatial distribution according to the land surface heterogeneity in the field.

In agricultural applications it is important to retrieve water availability data at finer resolution because soil moisture variability at a small scale can affect agricultural productivity. Thus the available SMAP L4_SM products would be more relevant for agricultural applications if the root zone soil moisture information would be available at a finer resolution. The study area of Twente region consists of many small agricultural fields with much variation in cropping pattern and vegetation type even within a small area of a few hectares. Thus, in this study a 50 m resolution is selected to obtain the final soil moisture maps. In 50 m resolution maps a better representation of the land surface details can be achieved for Dutch agricultural fields along with the average estimates of soil moisture in the field scale which can be relevant for agricultural applications.

1.3. Objectives

The main objective of this study is to quantify root zone soil moisture at a spatial resolution relevant for agricultural application through downscaling of the SMAP level 4 Soil Moisture (L4_SM) product using Sentinel-1 SAR.

The specific objectives of this study are as follows:

- I. To develop a method for downscaling the SMAP L4 surface soil moisture product using the Sentinel-1 SAR data.
- II. To identify a functional relationship between the SMAP L4 surface and root zone soil moisture for the study area to translate the downscaled surface data into a downscaled root zone product.
- III. To assess the accuracy of downscaled soil moisture products using in-situ measured surface and root zone soil moisture.

1.4. Research Questions

The following research questions can be formulated to address the specific objectives:

1. How can the impact of surface roughness, vegetation and incidence angle on Sentinel-1 SAR backscatter be considered and most effectively mitigated to downscaled surface soil moisture estimates?
2. What is the statistical relationship between the surface and root zone soil moisture embedded within the SMAP L4 products?
3. Does the downscaled surface and root zone soil moisture product meet the accuracy requirement of $0.04 \text{ m}^3 \text{ m}^{-3}$ unbiased Root Mean Square Error (ubRMSE) when compared to in-situ measurements?

1.5. Thesis Structure

The structure of this thesis is arranged in nine chapters. Chapter 1 gives the overall scientific background along with the main and specific objectives of this study. The description of the study area and the ancillary datasets are presented in Chapter 2. The satellite products used in this study is explained in Chapter 3. The general idea of the methodology and the steps followed to address the research problem and objectives of this study is explained in Chapter 4. The relationships developed and used for downscaling SMAP L4_SM is provided in Chapter 5. The results of validation of retrieved soil moisture with in-situ measurements are explained in Chapter 6. The downscaled soil moisture maps are presented in Chapter 7. In Chapter 8 factors affecting the sensitivity of backscatter from Sentinel-1 SAR to soil moisture is discussed and in chapter 9 based on the results and the limitations presented in this study, conclusions are drawn.

2. STUDY AREA AND DATA SETS

2.1. Twente region

The study area is the Twente region which lies in the eastern part of the Netherlands. The geographic coordinates of this region is 52°06' - 52°30' N latitude and 6° 15' -7°05'60" E longitude. Twente region lies in the eastern part of Overijssel province of the Netherlands with almost a flat terrain with highest elevation up to 50m above mean sea level (Dente, Vekerdy, Su, & Ucer, 2011). Figure 1 shows the location of the study area in the Netherlands and its topography.

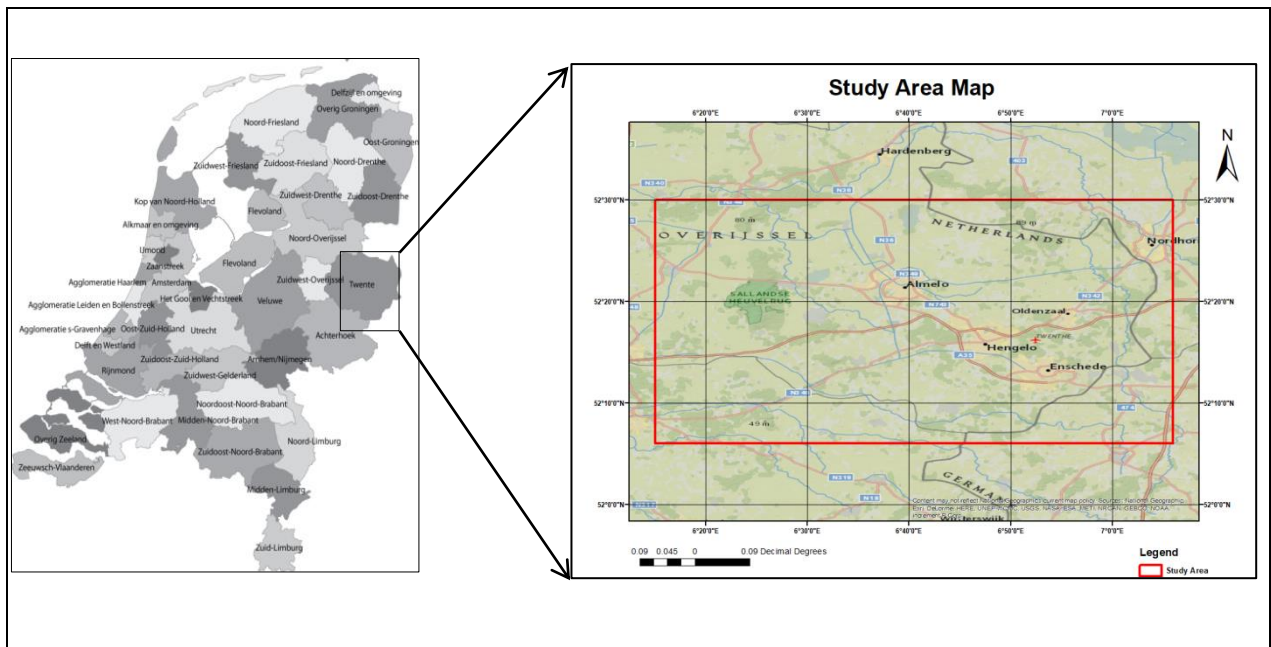


Figure 1: Location of Twente inside the Netherlands and map of the Twente region

The climate of this region is oceanic, with mild summers and mild winters. In 2016 temperature varied from a minimum monthly average temperature of 3.3°C in January to maximum monthly average temperature of 18.1°C in July. The rainfall is distributed relatively homogeneously throughout the year. In the year of 2016 the total average annual rainfall was 716 mm. Figure 2 shows the dynamics of rainfall pattern that occurred in the year of 2016 where we can see that maximum average daily rainfall was recorded up to 31 mm in May. This rainfall data is obtained from the #290 Twente station and acquired from the Royal Netherlands Meteorological Institute (KNMI) website (<http://www.knmi.nl/nederland-nu/klimatologie>).

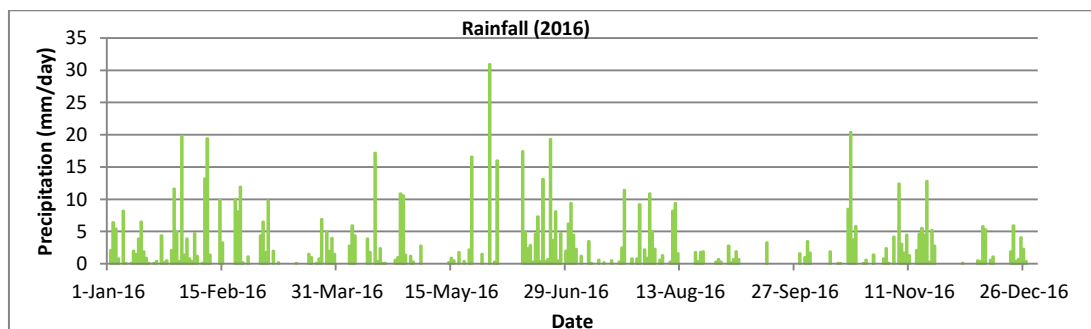


Figure 2: The dynamics of rainfall pattern in Twente region for the year 2016.

2.2. Datasets

2.2.1. Land Cover data

Basic Registration of Crop Parcel (BRP) is the data portal of Dutch government and consists of data about the crops cultivated in the agricultural areas, at parcel level in Netherlands (<https://data.overheid.nl/data/dataset/basisregistratie-gewaspercelen-brp>). A land cover class data of the study area for the period of 2016 has been retrieved from the same portal (Dataportal of the Dutch government, 2016). Figure 3 shows the land cover classes of the study area with a very high land surface heterogeneity consisting of several urban areas, forest patches and mosaic of agricultural fields (mainly grasslands and croplands).

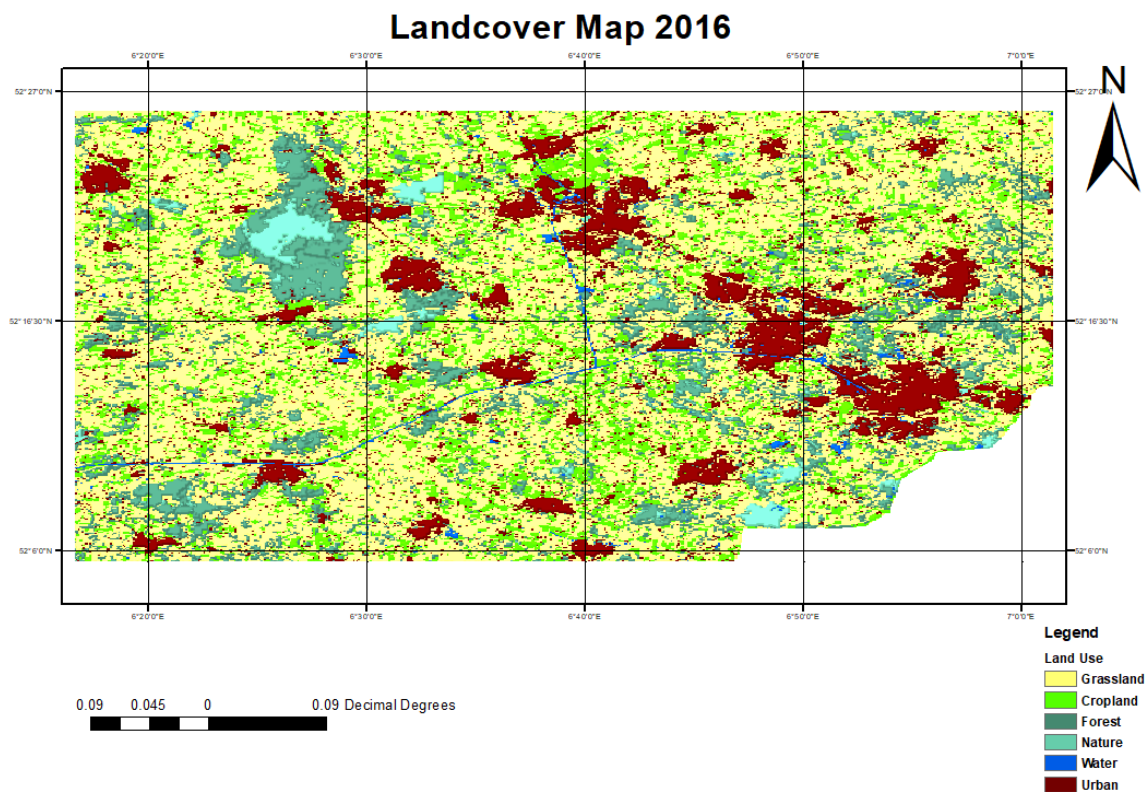
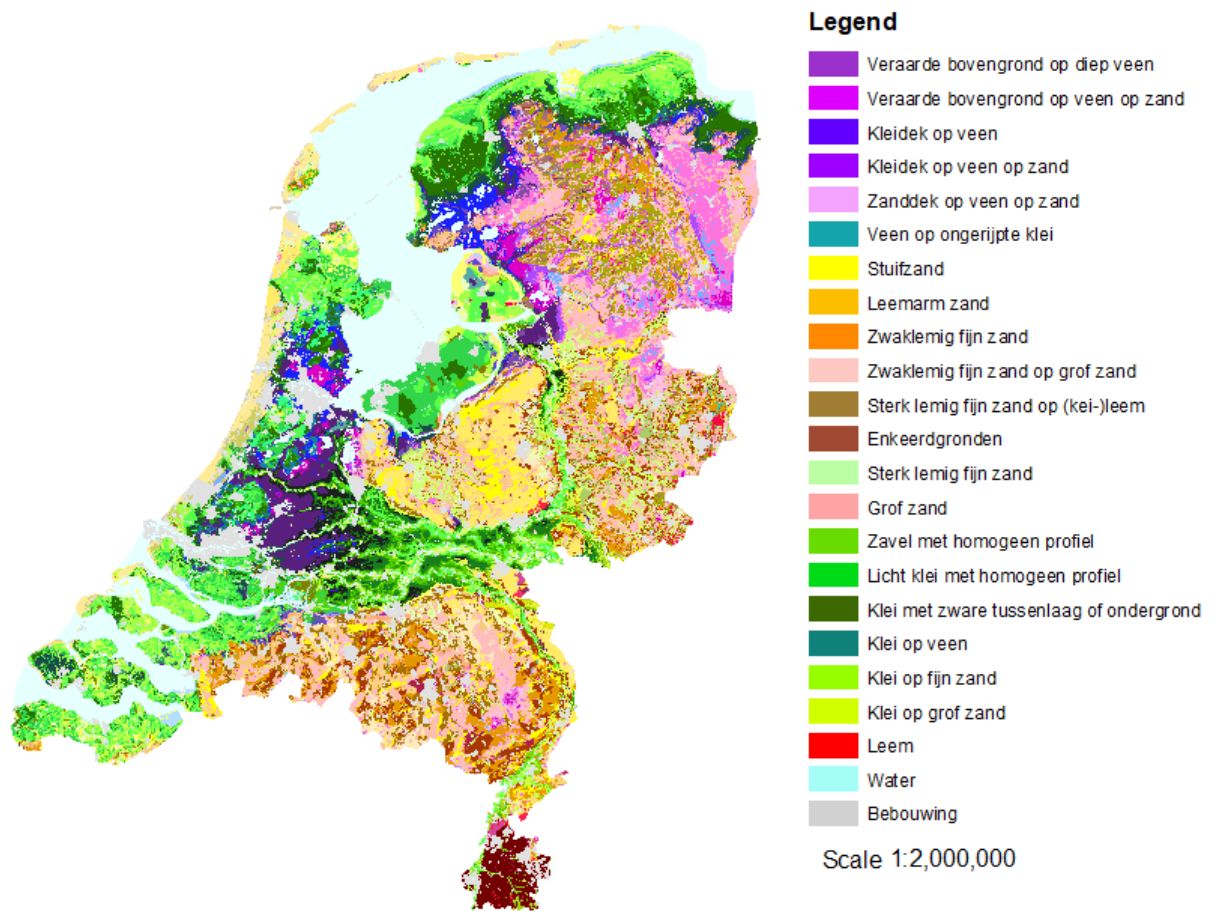


Figure 3: Land cover map of 2016 showing the different land cover classes of the Twente region.

2.2.2. Soil Properties data

The water holding capacity of the soil plays an important role when it comes to quantifying soil moisture distribution. A soil physics unit map called BODEMFYSISCHE EENHENDENKAART (BOFEK2012) is used in this study which is obtained from the website of Wageningen University and Research, WUR (<https://www.wur.nl/nl/show/Een-nieuwe-bodemfysische-schematisatie-van-Nederland.htm>). Figure 4 shows the soil physical unit map of the Netherlands. These soil properties maps are obtained at a resolution of 250m. In this map it can be seen that the study area of the Twente region mainly consists of sandy ('zand' in the legend) and loamy ('leem' in the legend) soils.



(Source: <https://www.wur.nl/nl/show/Een-nieuwe-bodemfysische-schematisatie-van-Nederland.htm>)

Figure 4: The soil unit properties map for Netherlands obtained from BOFEK2012.

2.2.3. In-situ measurement data

In 2008 and 2009, the Faculty of Geo-information Science and Earth Observation (ITC) of the University of Twente placed 20 soil moisture and soil temperature monitoring stations in the Twente region out of which 16 stations are placed in the grass land, 3 in corn field and 1 in forest (Dente et al., 2011). Figure 5 shows the location of the 20 soil moisture monitoring stations over the study area of Twente distributed with an extent of 50 km * 40 km.

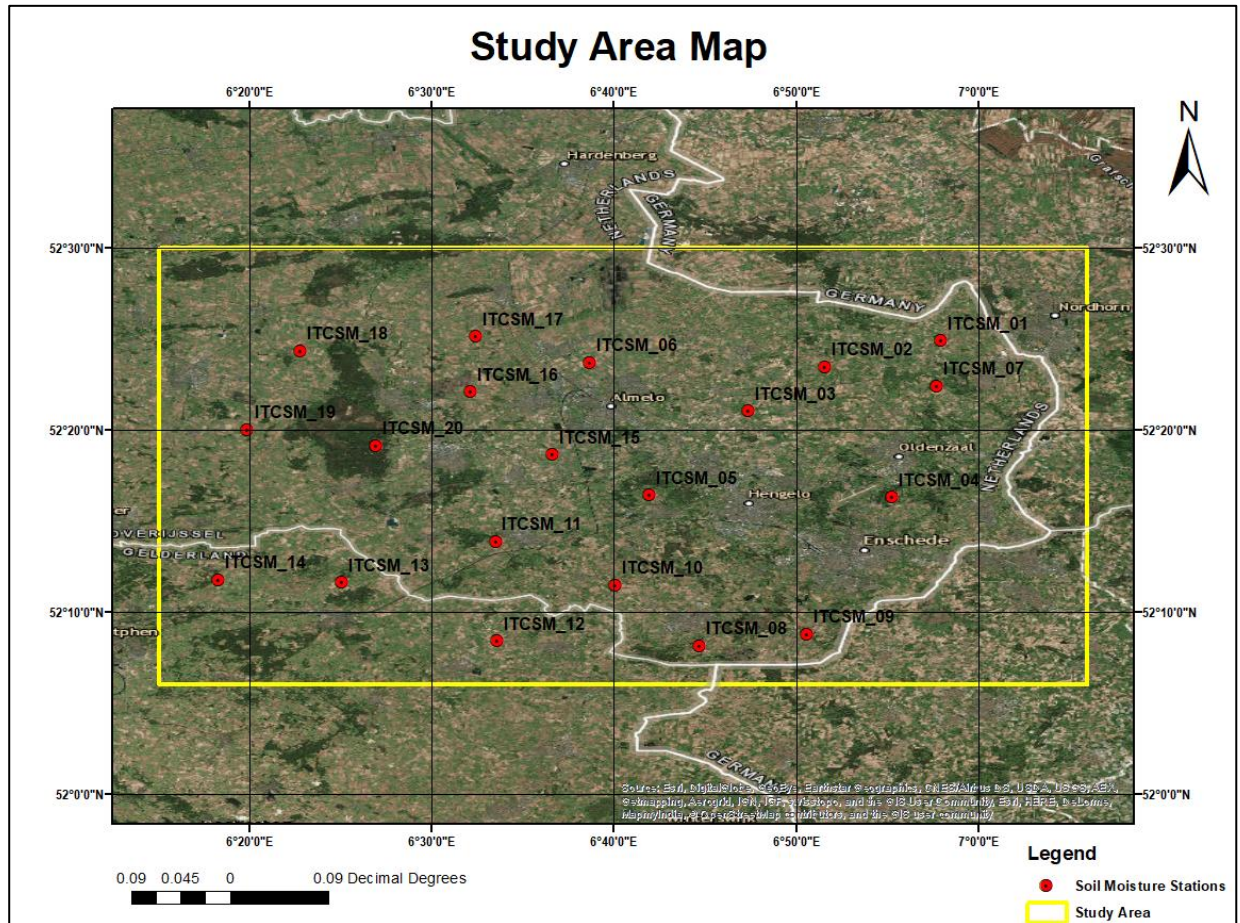


Figure 5: Google earth image showing the study area of Twente and red dots shows the distribution of the 20 soil moisture measurement stations placed by the ITC in twente region.

Each monitoring stations consists of one Em50 ECH₂O data logger which records data collected by two to five EC-TM ECH₂O probes (Dente et al., 2011). Figure 6 shows the stations in the study area which gives the measure of volumetric soil moisture for nominal depth of 5cm, 10cm, 20cm, 40cm and 80cm below the surface for every 15 minutes. The soil moisture data downloaded from these stations are used for the validation of the downscaled surface and root zone soil moisture.

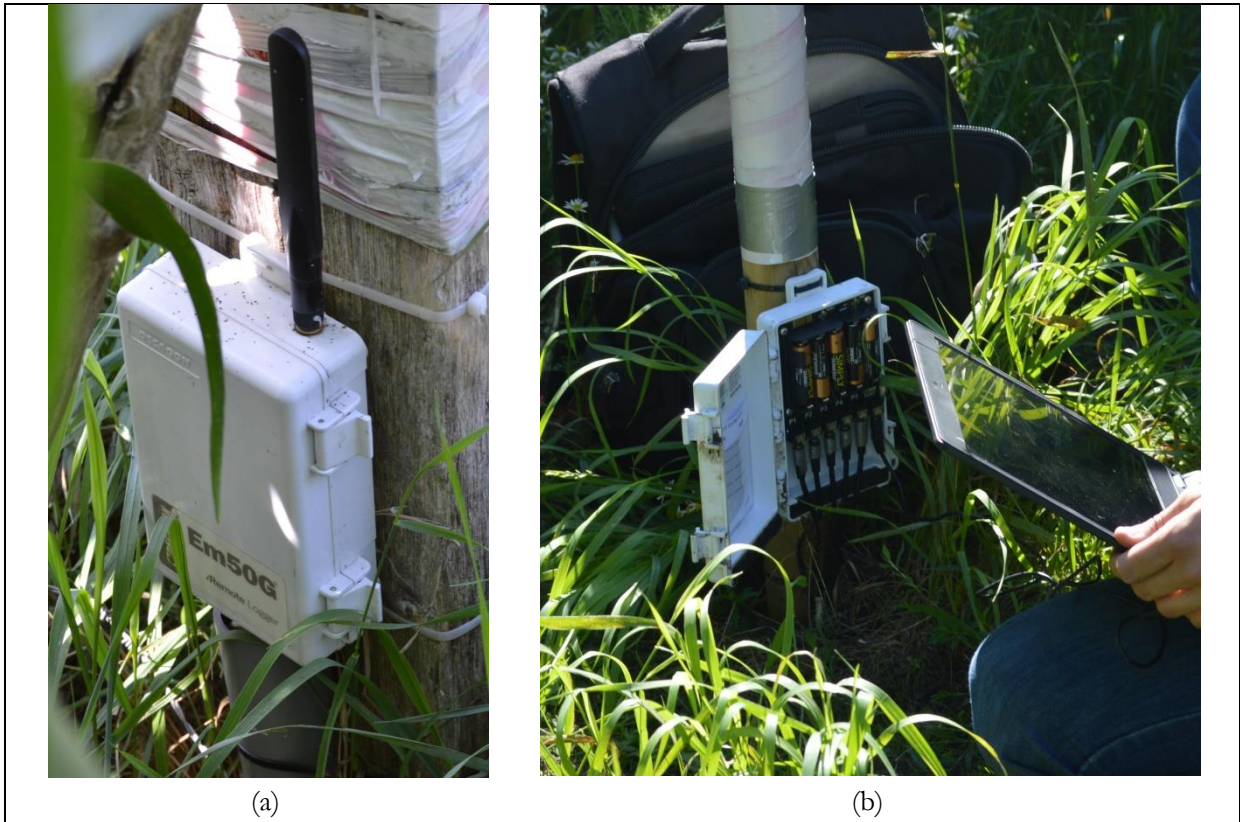


Figure 6: (a) is sample of soil moisture monitoring station in the study area and (b) shows the data recorded by this station being downloaded.

3. SATELLITE PRODUCTS

3.1. SMAP L4_SM product

SMAP L4_SM products are available since 31 October 2015 and can be downloaded from National Snow and Ice Data Centre (NSIDC; http://nsidc.org/data/docs/daac/smap/sp_l4_sm/index.html). These products are the result of the assimilation of SMAP brightness temperature into the Goddard Earth Observation Model System, Version-5 (GEOS-5) based catchment land surface model (Koster et al., 2000). The model is driven by the surface meteorological forcing data including precipitation as the most important driver for soil moisture (Reichle et al., 2016). These precipitation data are observation based and hence act as a realistic forcing providing some initial reliability in the model simulation (SMAP Science Team, 2014). The model also considers the key land surface processes and also the vertical transfer of soil moisture across the root zone. The model conserves both water and energy balance by dividing precipitation into runoff, recharge and evaporation and incident radiation into outgoing radiation sensible and latent heat fluxes. The final product obtained from this assimilation is the soil moisture estimates at 9 km resolution for every three hours. These SMAP L4_SM are the model-derived value-added products, that gives the estimates of both surface soil moisture (for 5 cm depth of the soil surface) and root zone soil moisture (for 1 m depth of the soil surface) and are grouped into three products files (NSIDC, 2015).

- i. Geophysical Data provides soil temperature, soil moisture and land surface fluxes data. These are the time-averaged geophysical data.
- ii. Analysis Update Data provides the instantaneous data which are obtained after the ensemble Kalman filter analysis update. These data comprises of soil moisture and temperature estimate along with the estimates of their corresponding uncertainties.
- iii. Land Model Constants are the data that provides the time-invariant model parameters used in the Catchment land surface model.

In this study, the Analysis Update Data of SMAP L4_SM product is used for downscaling. These products were downloaded from the website of NSIDC for the year 2016. The SMAP L4_SM products are available with a temporal resolution of 3 hours giving 8 data per day but in this study, the data only for 6 am and 6 pm for the year 2016 has been extracted. This was done so that all available Sentinel-1 SAR data for 2016 would correspond to SMAP L4_SM product giving sufficient data for soil moisture analysis as Sentinel-1 SAR provides data at 6 am (descending pass) or 6 pm (ascending pass). These SMAP products cover the study area in with 24 pixels as shown in Figure 7. Each SMAP pixel gives the estimate for the surface and root zone soil moisture content.

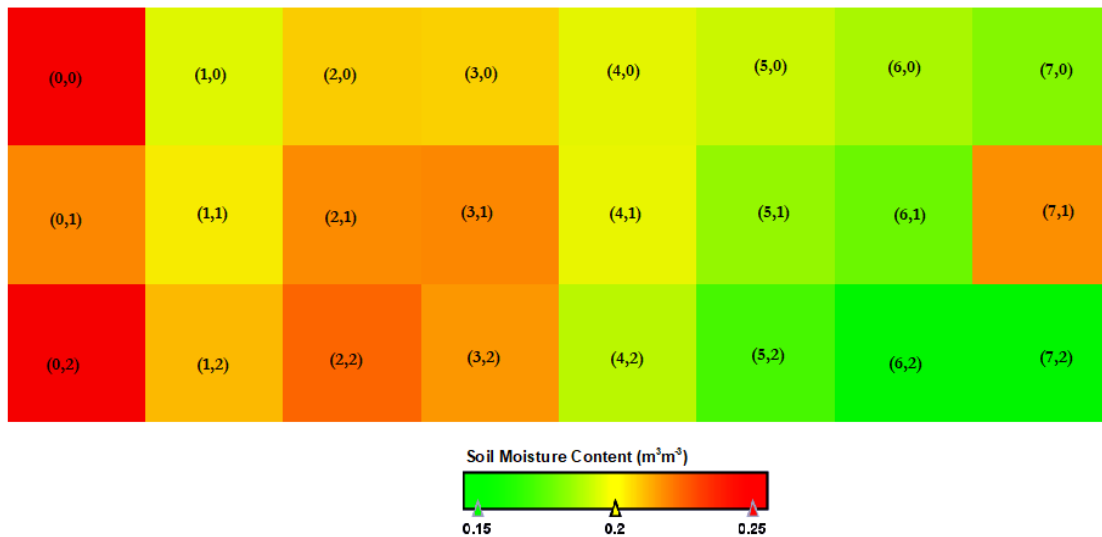


Figure 7: SMAP L4 image of 1st January 2016 in the study area of the Twente region which gives the estimates of soil moisture content in each pixel.

3.2. Sentinel-1 SAR

Sentinel-1 is a two satellite constellation which provides operational Synthetic Aperture Radar (SAR) data. Sentinel-1 operates at the frequency of 5.405 GHz, which has the potential to penetrate through the clouds and provide continuous imagery in all-weather conditions and at both day and night time (Sentinel 1 Team, 2013). In this study the Level-1 Interferometric Wide Swath (IW) Sentinel-1 Ground range detected (GRD) SAR data are used. For the study area the images in IW can be retrieved at a temporal resolution of 2-6 days and spatial resolution of 10m. These data can be downloaded from Sentinels Scientific Data Hub (<https://scihub.copernicus.eu/dhus/#/home>). The available data set consists of 133 Sentinel-1 images of the Twente region for the year 2016. Some of the main characteristics of Sentinel-1 SAR data used in this study are shown in Table 1 below.

Table 1: Characteristics of high resolution Level-1 IW Sentinel-1 (Sentinel 1 Team, 2013)

Characteristics	High Resolution Interferometric Wide Swath
Incidence Angle range	29.1°-46°
Wavelength	C-band (5.405 GHz)
Polarization	Dual VV+VH (over land)
Temporal Resolution	2-6 days (for the study area)
Pixel Resolution	10 m × 10 m
Orbital Pass	Four orbital passes (15, 37, 88 and 139)

After downloading the Sentinel-1 images from the website, some pre-processing is needed before they can be used. The pre-processing of the Sentinel-1 SAR images was done by a colleague, Ir. H.F. Benninga (PhD student). Figure 8 shows a sample image of pre-processed Sentinel-1 SAR of 7th January 2016. The executed pre-processing steps are as follows:

- Sentinel Application platform (SNAP) software was used for the terrain correction of the images. Terrain correction was done by orthorectification and radiometric normalization to correct the distortions in the image. The range Doppler Terrain Correction tool was used for this purpose.

This process also created three bands in the image giving band 1 as backscattering at horizontal polarization (σ_{VH}) in intensity ($\text{m}^2 \text{m}^{-2}$) which is converted into decibels (dB), band 2 as backscattering at vertical polarization (σ_{VV}) in intensity ($\text{m}^2 \text{m}^{-2}$) which is converted into decibels (dB) and band 3 as the incidence angle corrected for the local slope in degrees.

- The images that completely or partly overlap the study area were downloaded so the subset tool was used to extract only the required area of our study.
- Sometimes the combination of two or more images gave the complete coverage of the study area. So these images were combined to get the complete study area in one image.
- Speckle filtering was used to remove the noise in the images. A Median Filter with a 5×5 window size was used for filtering speckle.

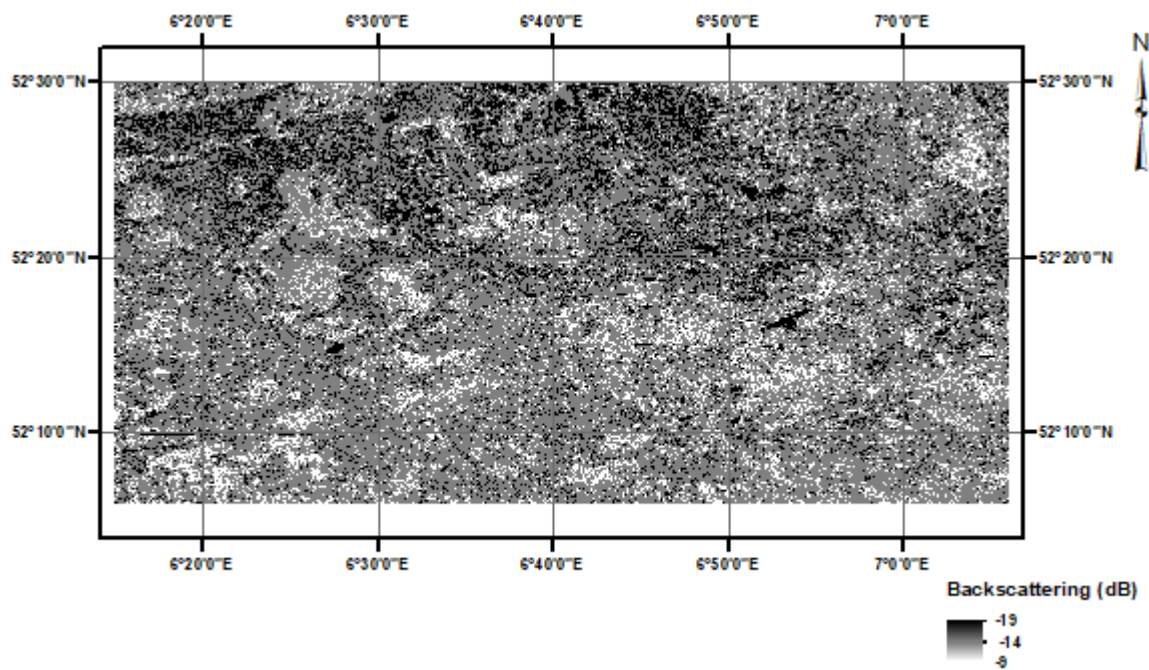


Figure 8: A sample image of Sentinel-1 SAR showing the region of Twente and acquired on 7th January 2016 after the completion of pre-processing steps.

4. RESEARCH METHODOLOGY

4.1. Methodology Flowchart

Figure 9 summarizes the general idea of the methodology involved in this research. An empirical relationship between the SMAP L4 surface soil moisture index and root zone soil moisture index were developed. The Sentinel-1 SAR backscatter data were aggregated to coarser (i.e. 9 km) and medium (i.e. 50 m) resolution. The coarse resolution backscatter data were correlated with SMAP surface soil moisture index to get the soil sensitive parameter. This parameter was used with SMAP downscaling algorithm with the medium resolution backscatter data and coarse resolution SMAP surface soil moisture index to retrieve downscaled surface soil moisture index at a medium resolution. This downscaled surface soil moisture index was then used with the relationship obtained between SMAP surface and root zone soil moisture index to get downscaled root zone soil moisture index. The downscaled surface and root zone soil moisture index were rescaled to surface and root zone soil moisture content. The resulting downscaled surface and root zone soil moisture were validated with the in-situ measurements obtained from soil moisture monitoring stations in the Twente region.

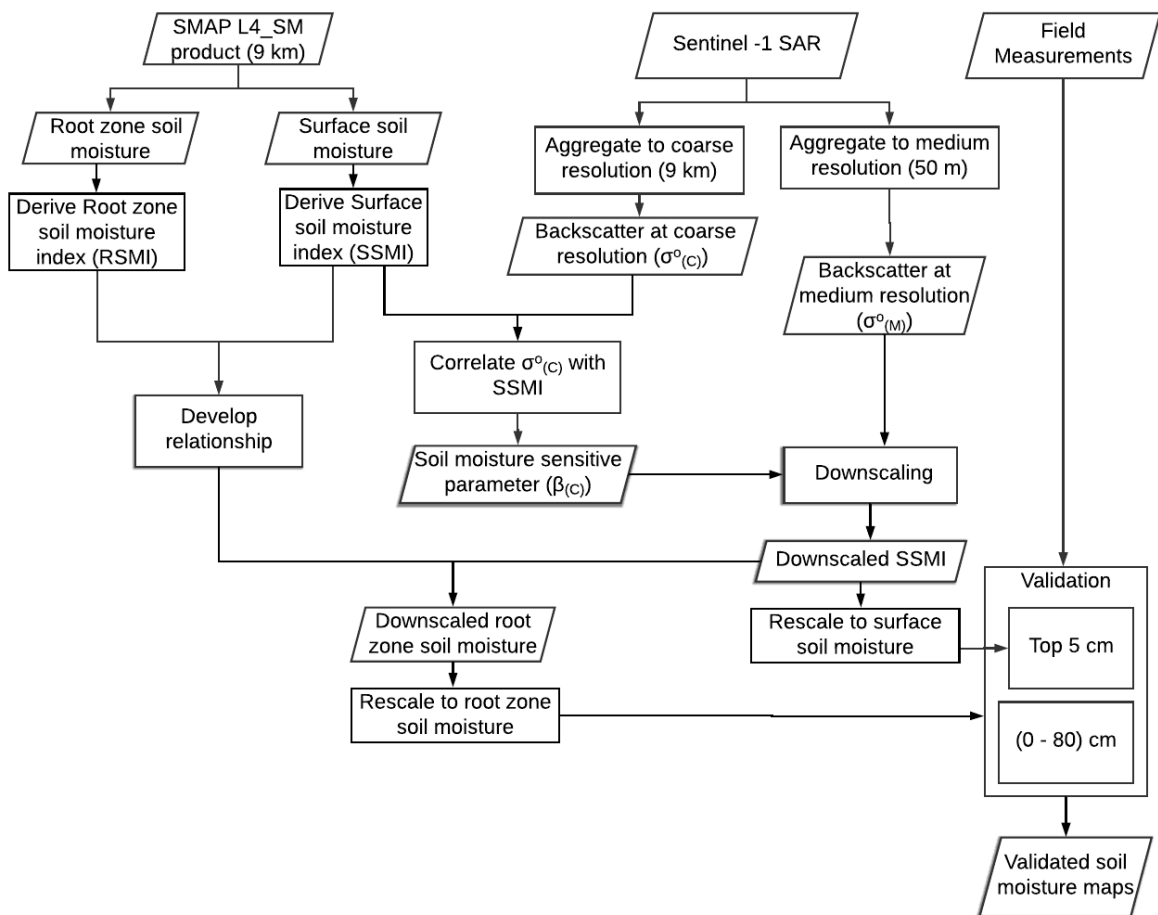


Figure 9: A schematic representation of the procedures involved in combining SMAP L4_SM product and Sentinel-1 SAR data to retrieve downscaled surface and root zone soil moisture product.

4.2. Translating SMAP L4 Soil moisture into Soil Moisture Index

To downscale root zone soil moisture, it is also important to consider soil texture properties as it plays an important role in the soil moisture variability. In a study done in Arizona by English et al., (2005), they have described how soil moisture content varies and how it is affected by the different soil types. Soil properties affect the vertical movement of water in the soil as different types of soil have different water holding and releasing capacity (Li et al., 2014) affecting the moisture conditions at different depths. These moisture conditions can be normalized for differences in minimum (wilting point) and the maximum (saturated water content) by the help of Soil Moisture Index (SMI). SMI gives the values between 0 to 1, where 0 means dry and 1 means wet soil.

SMAP L4_SM is a modelled product and includes the soil physical parameters, the model parameters (porosity and wilting point) used in the model assimilation are at a coarser resolution of 9 km. In this study these model parameters retrieved from Land Model Constants data of SMAP L4_SM product are used to translate the surface and root zone soil moisture into Soil Moisture Index (SMI). These SMI data is downscaled to a finer resolution and rescaled back to volumetric soil moisture estimates on the basis of soil physical characteristics from BOFEK2012. This will also incorporate information about soil properties in downscaling procedure. Thus, in this study the SMAP soil moisture content for surface (at a depth of 0 to 5 cm) and root zone (at a depth of 0 to 1 m) are converted into SMI using the porosity and the wilting point. The Surface Soil Moisture Index (SSMI) was calculated using the relationship as explained by Sánchez et al., (2016)

$$SSMI = \frac{\theta - \theta_{\min}}{\theta_{\max} - \theta_{\min}} \quad (1)$$

Where θ is the surface soil moisture estimates in m^3m^{-3} obtained from SMAP, θ_{\min} is the moisture at the wilting point for surface soil moisture in m^3m^{-3} and θ_{\max} is the porosity for surface soil moisture in m^3m^{-3} and are included in the Land Model Constants data obtained from NSIDC.

The similar relationship (i.e. equation 1) is used for calculating Root zone Soil Moisture Index (RSMI) where θ will be the root zone soil moisture estimates in m^3m^{-3} obtained from SMAP. The value of θ_{\min} and θ_{\max} will be taken as the moisture at the wilting point for root zone soil moisture in m^3m^{-3} and the porosity for root zone soil moisture in m^3m^{-3} respectively obtained from the Land Model Constants data.

4.3. Downscale surface soil moisture index

The downscaling of coarse resolution surface soil moisture index is done based upon the Baseline algorithm for SMAP proposed by Das et al. (2011). The algorithm is based on a linearized relationship between radar backscattering and radiometer volumetric soil moisture content. This relationship has been discussed by Kim & van Zyl (2009) where they found a near-linear relationship during the Washita 92 field experiment and by Narayan et al. (2006) where they reported a linear relation between radar backscatter and volumetric soil moisture content in the Soil Moisture Experiment 2002 (SMEX02). Based on this approach final combined product obtained from this algorithm is the volumetric soil moisture at a medium resolution. The mathematical formulation of this algorithm is shown below:

$$SSMI_{(M)} = SSMI_{(C)} + \beta_{(C)} \times \{\sigma^o_{(M)} - \sigma^o_{(C)}\} \quad (2)$$

Where at a given time, $SSMI_{(C)}$ is the coarser soil moisture index obtained from SMAP as explained in Section 4.2, $\sigma^o_{(M)}$ and $\sigma^o_{(C)}$ are obtained from aggregated SAR data to medium and coarser resolution respectively in dB and $SSMI_{(M)}$ is the required soil moisture index in a medium resolution and is unitless. M represents the variables in medium resolution which is our targeted resolution (i.e. 50 m) for final soil

moisture maps and C represents the variable in coarse resolution which is the resolution of original SMAP L4 soil moisture product (i.e. 9 km) and $\beta_{(C)}$ is in dB^{-1} and is obtained from the linearized relationship between SSMI and backscattering.

Radar backscatter vs. SSMI relationship

A linear relationship is assumed between the radar backscattering coefficient and SMAP surface soil moisture in the downscaling algorithm used in this study. Since, we have linearly transformed SMAP soil moisture to soil moisture index, similar relationship is expected in this study between the radar backscattering coefficient and SMAP surface soil moisture index too. The aggregation of SAR also reduces the speckle effect in the image. This aggregated backscattering of Sentinel-1 SAR is used in the SMAP baseline algorithm shown in equation (2) to downscale SMAP SSMI from 9 km to a resolution of 50 m. A linear regression between the aggregated Sentinel-1 SAR data to a resolution of 9 km and SMAP SSMI is performed and the relationship obtained is as shown in equation (3).

$$SSMI_{(C)} = \alpha_{(C)} + \beta_{(C)} * \sigma^o_{(C)} \quad (3)$$

The $\beta_{(C)}$ and $\sigma^o_{(C)}$ obtained from this equation is used in the downscaled algorithm shown in equation (2).

Then Sentinel-1 SAR data is again aggregated to a medium resolution of 50 m so that backscattering obtained at this resolution, $\sigma^o_{(M)}$ can also be used in the downscaling algorithm. But before aggregating SAR to 9 km or 50 m, the backscattering signals over urban and forest areas which can affect the soil moisture estimation were removed by masking out the forest and urban areas.

Normalizing Incidence Angle effect

The view angle of Sentinel-1 SAR data ranges from 29.1° to 46° (Sentinel 1 Team, 2013) which affects the interpretation of backscatter values. So, before performing linear regression, the effect of variation of incidence angle on backscattering is needed to be compensated and can be done by normalizing the backscattering towards a reference angle. The most commonly used method is by applying Lambert's scattering law (Mladenova et al., 2013).

$$\sigma^o_{ref} = \sigma^o * \frac{\text{Cos}^n(\theta_{ref})}{\text{Cos}^n(\theta_V)} \quad (4)$$

Where σ^o_{ref} is the normalized backscattering coefficient in dB, θ_{ref} is the reference view angle in degrees, θ_V is the view angle in degrees and n depends upon the type of scattering and varies according to the type of land cover.

4.4. Downscale root zone soil moisture index

The downscaling of root zone soil moisture index in this study is based on the assumption that the relationship between surface soil moisture and root zone soil moisture obtained at coarse resolution is same for finer resolution that leads to downscaled root zone soil moisture. Thus, a statistical relationship between the SSMI and RSMI at 9 km resolution was established. This relationship is used with downscaled surface soil moisture to retrieve root zone soil moisture product at a finer resolution. Following relationship was used to rescale SMI to soil moisture.

$$\theta = SMI (\theta_{max} - \theta_{min}) + \theta_{min} \quad (5)$$

Where, in case of surface soil moisture, SMI refers to SSMI, θ_{max} represents the saturated soil moisture ($\text{m}^3 \text{m}^{-3}$) for 5 cm soil depth and θ_{min} represents the moisture content at wilting point ($\text{m}^3 \text{m}^{-3}$) of the 5 cm

soil depth. For root zone soil moisture SMI refers to RSMI, θ_{max} represents the saturated soil moisture (m^3m^{-3}) for 100 cm soil layer and θ_{min} represents the moisture content at wilting point (m^3m^{-3}) of the 100 cm soil layer. The data for θ_{max} and θ_{min} are obtained from the BOFEK2012. For θ_{max} 1 cm pressure head (i.e. $\text{pF} = 0$) is considered and for θ_{min} 16000 cm pressure head (i.e. $\text{pF} = 4.2$, equivalent to wilting point)

4.5. Errors metrics

The resulting downscaled SMAP products are validated against in-situ measurements to assess its accuracy. The soil moisture data retrieved from remote sensing and field measurements have different statistical characteristics. These statistical discrepancies are manifested in a bias between the observed and in-situ measured data that has to be considered while assessing accuracy. So, to remove these biases the retrieved soil moisture data were normalised using the standard deviation and mean values, taking the field data as a reference.

$$\theta'_R = \mu_M + (\theta_R - \mu_R) * \left(\frac{\sigma_M}{\sigma_R}\right) \quad (6)$$

Where, θ'_R is the retrieved soil moisture rescaled to field measurements in m^3m^{-3} , σ_R represents the standard deviation of retrieved soil moisture observation rescaled to field measurements data in m^3m^{-3} and σ_M represent the standard deviation of in-situ measurements in m^3m^{-3} . μ_M represents the mean value of field measurements in m^3m^{-3} and μ_R represents the mean value of retrieved soil moisture observation rescaled to field measurements data in m^3m^{-3} .

After bias correction, the unbiased Root Mean Squared Error (ubRMSE) was calculated to see the matchups between the retrieved soil moisture and in-situ measurements. The ubRMSE was calculated as (Zhang et al., 2017):

$$\text{ubRMSE} = \sqrt{\frac{1}{N} \sum_{i=1}^N (\theta'_R(i) - \theta_M(i))^2} \quad (7)$$

The coefficient of determination (R^2) was calculated as:

$$R^2 = \left(\frac{\sum_{i=1}^N (\theta'_R(i) - \mu_R) - (\theta_M(i) - \mu_M)}{(N-1) * \sigma_R * \sigma_M} \right)^2 \quad (8)$$

Where, θ_M is the field measurements of soil moisture in m^3m^{-3} , N is the total number of time steps and i represent the specific time steps.

5. DEVELOPMENT OF RELATIONSHIPS

5.1. Sentinel-1 SAR backscatter vs SMAP L4 SSMI

The SMAP soil moisture estimates were translated into soil moisture index using the relation discussed in Equation (1) of Section 4.1. These soil moisture indices for surface and root zone were extracted to further develop the relationships. The backscatter observations from Sentinel-1 SAR in the study area were aggregated to 9 km resolution resulting in 24 pixels over the Twente region for each satellite image. Scatter plots of the aggregated backscatter for VH polarization (σ°_{VH}) and for VV polarization (σ°_{VV}) with SSMI were created and linear relationship was fitted for each pixel. Hence, 24 different relationships of SSMI with σ°_{VH} and σ°_{VV} were created. The pixel containing station 04 which is pixel (7,1), was selected for further analysis because it showed the highest correlation R^2 among the 24 relationships (see Table 2 and Table 3). The result of the linear regression for pixel (7,1) is shown in Figure 10 where an expected linear relationship between backscatter data and SSMI is seen such that, in average for every 0.1 SSMI increment 1 dB increment is seen in backscatter observation. The sensitivity of backscatter to SSMI is defined by the parameter, $\beta_{(C)}$. For pixel (7,1) $\beta_{(C)}$ is obtained as 0.075 dB^{-1} for σ°_{VH} and 0.085 dB^{-1} for σ°_{VV} which shows σ°_{VV} to be slightly more sensitive to soil moisture. Although pixel (7,1) shows the highest value of R^2 among 24 relationships, a large spread is seen in Figure 10.

Table 2 shows the value of R^2 obtained from the relationship between SMAP SSMI and σ°_{VH} which range from 0.160 to 0.313 for all SMAP pixels and Table 3 shows the value of R^2 obtained from the relationship between SMAP SSMI and σ°_{VV} which range from 0.096 to 0.302. For all 24 pixels $\beta_{(C)}$ was found to be ranging from 0.031 dB^{-1} to 0.064 dB^{-1} for σ°_{VH} and from 0.085 dB^{-1} to 0.029 dB^{-1} for σ°_{VV} . This significant variation in $\beta_{(C)}$ for different pixels can be the impact of land surface heterogeneity over $\beta_{(C)}$ even when backscatter is aggregated to a resolution of 9 km.

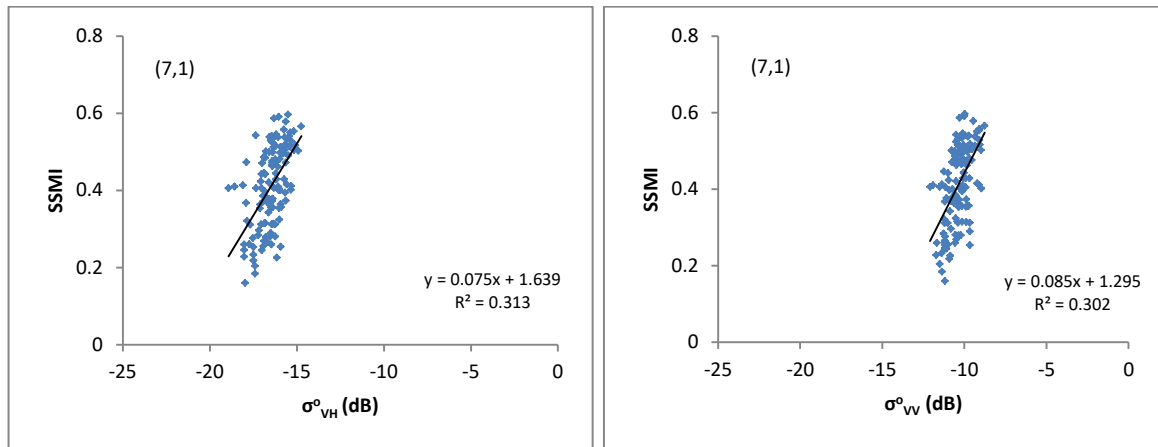


Figure 10: SMAP SSMI plotted against backscattering coefficient (σ°_{VH} and σ°_{VV}) for selected pixel (7,1).

Table 2: The parameters ($\alpha_{(C)}$ and $\beta_{(C)}$) for equation (3) and R^2 obtained from the linear relationship between aggregated σ°_{VH} and SMAP SSMI for all the 24 pixels in the study area. The bold values show the minimum and the maximum range of R^2 .

S No	Pixel	$\alpha_{(C)}$	$\beta_{(C)}$	R^2
1	(0,0)	1.586	0.064	0.169
2	(1,0)	1.226	0.046	0.161
3	(2,0)	1.318	0.051	0.197
4	(3,0)	1.176	0.042	0.162

5	(4,0)	1.234	0.047	0.184
6	(5,0)	1.131	0.039	0.187
7	(6,0)	1.135	0.040	0.190
8	(7,0)	1.179	0.043	0.227
9	(0,1)	1.576	0.062	0.227
10	(1,1)	1.380	0.053	0.212
11	(2,1)	1.364	0.053	0.165
12	(3,1)	1.239	0.045	0.143
13	(4,1)	1.248	0.047	0.189
14	(5,1)	1.313	0.054	0.218
15	(6,1)	1.329	0.055	0.251
16	(7,1)	1.639	0.075	0.313
17	(0,2)	1.387	0.052	0.206
18	(1,2)	1.455	0.058	0.212
19	(2,2)	1.480	0.056	0.211
20	(3,2)	1.254	0.045	0.171
21	(4,2)	1.085	0.036	0.160
22	(5,2)	1.099	0.038	0.235
23	(6,2)	1.050	0.036	0.260
24	(7,2)	0.979	0.031	0.221

Table 3: The parameters ($\alpha_{(C)}$ and $\beta_{(C)}$) for equation (3) and R^2 obtained from the linear relationship between σ_{VV} and SMAP SSMI for all the 24 pixels in the study area. The bold values show the minimum and the maximum range of R^2

S No	Pixel	$\alpha_{(C)}$	$\beta_{(C)}$	R^2
1	(0,0)	1.033	0.048	0.112
2	(1,0)	0.868	0.038	0.096
3	(2,0)	0.945	0.045	0.135
4	(3,0)	0.849	0.037	0.107
5	(4,0)	0.986	0.051	0.176
6	(5,0)	0.927	0.042	0.173
7	(6,0)	0.936	0.043	0.177
8	(7,0)	0.958	0.045	0.194
9	(0,1)	0.931	0.038	0.102
10	(1,1)	0.891	0.037	0.107
11	(2,1)	0.941	0.043	0.101
12	(3,1)	0.922	0.041	0.098
13	(4,1)	0.960	0.046	0.147
14	(5,1)	1.046	0.062	0.217
15	(6,1)	1.071	0.063	0.236
16	(7,1)	1.295	0.085	0.302
17	(0,2)	0.931	0.038	0.114
18	(1,2)	0.959	0.043	0.111
19	(2,2)	1.025	0.046	0.132
20	(3,2)	0.936	0.040	0.113
21	(4,2)	0.836	0.034	0.116

22	(5,2)	0.932	0.044	0.225
23	(6,2)	0.825	0.035	0.201
24	(7,2)	0.763	0.029	0.156

Incidence angle effect

In general the available Sentinel-1 SAR images for 2016 from different orbits showed the variation of incidence angle ranging from 34° to 44° in this study. This variation in incidence angle can affect the backscatter data and can ultimately cause variation in $\beta_{(C)}$ which needs to be investigated. The variation in the incidence angle was normalized to a reference angle of 40° based on the Lamberts cosine law as explained in equation (4) of Section 4.3. The value of n was taken as 1 assuming a volume scattering, following Van der Velde et al., (2014) for the same study area. This normalized backscatter was plotted against SSMI as shown in Figure 11 where some improvement was seen in R^2 for pixel (7,1) when compared with previous result (Figure 10), an increment from 0.313 to 0.418 for VH and from 0.302 to 0.374 for VV is seen.

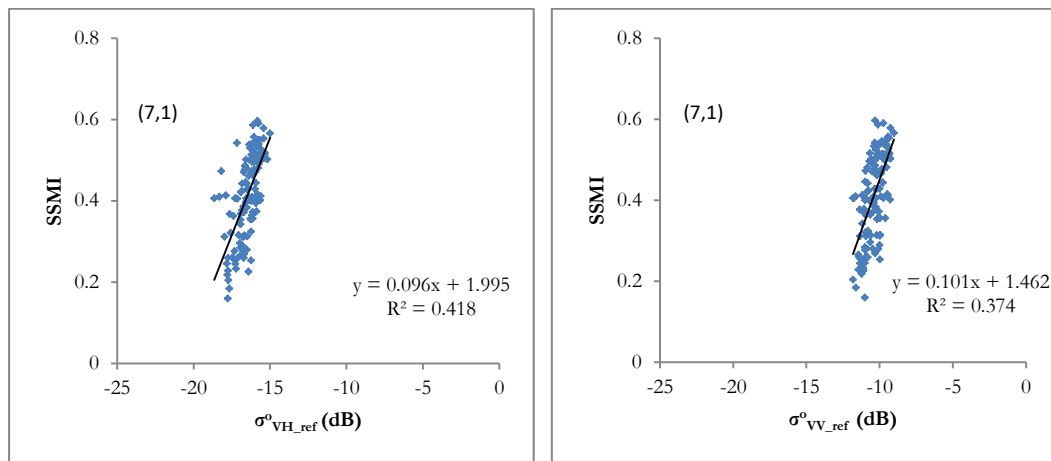
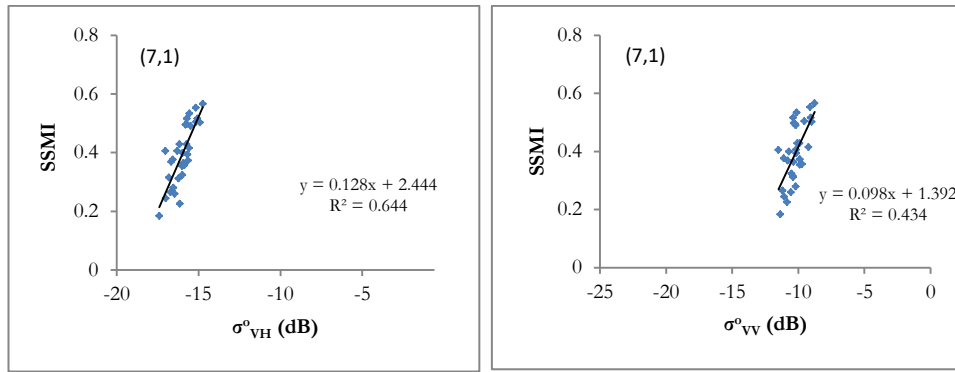


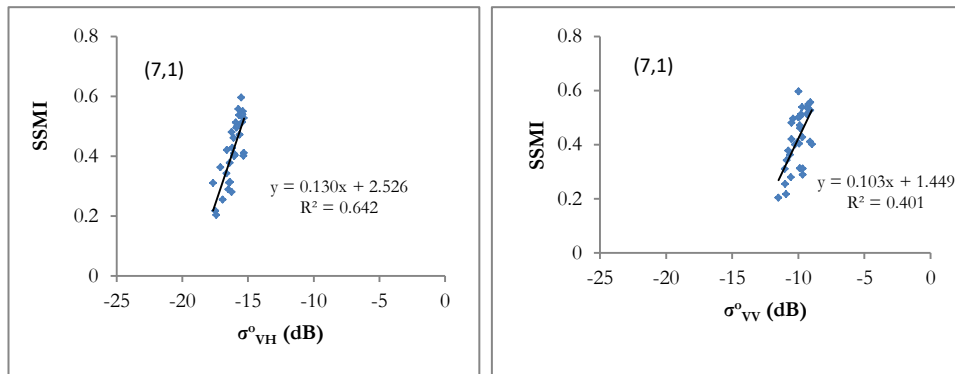
Figure 11: SMAP SSMI plotted against the normalized backscattering coefficient ($\sigma^{\circ}_{VH_ref}$ and $\sigma^{\circ}_{VV_ref}$) for the selected pixel (7,1).

View angle correction showed some improvement in R^2 , but was still low. So, to obtain a better relationship, instead of view angle correction, the Sentinel-1 SAR backscatter images were separated according to their orbital passes. When Sentinel-1 SAR backscatter data were separated according to the dates of different orbital passes (15, 37, 88 and 139) and the relationships were analysed, a significant improvement in R^2 was seen. Separating the orbital passes also separates the incidence angles, and gives a larger improvement than by normalizing the incidence angle. The scatter plot for all orbital passes of the selected pixel (7,1) containing station 04 is shown in Figure 12.

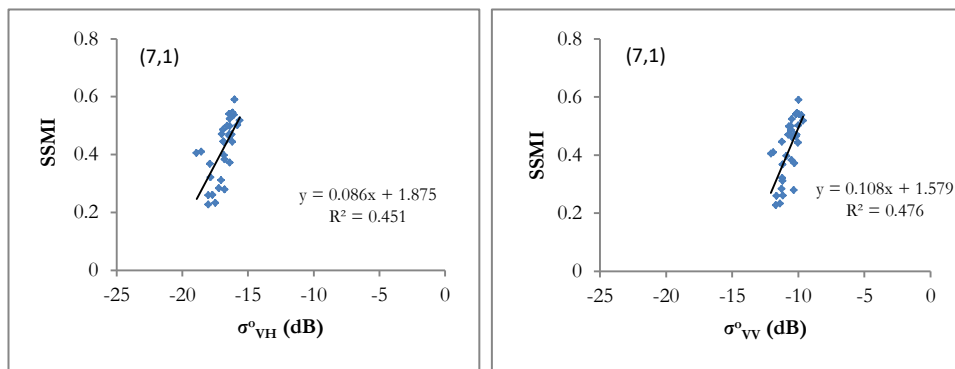
Orbit 15 (incidence angles of 33° - 35°) showed better correlation when compared to orbit 139 (incidence angles of 42° - 45°). A similar result was obtained by Calvet et al., (2011), where the C-band sensitivity towards soil moisture decreased for higher incidence. Thus, to remove the effect of incidence angles on backscatter sensitivity to soil moisture different values of $\beta_{(C)}$ for different orbits were considered in this study, as shown in Table 4 and Table 5. In these tables we can see that the significant variation of $\beta_{(C)}$ still exists among the SMAP pixels. In general Table 4 and Table 5 shows that in average for all orbits R^2 varies from 0.035 dB^{-1} to 0.131 dB^{-1} for σ°_{VH} and from 0.029 dB^{-1} to 0.131 dB^{-1} for σ°_{VV} . These variations in $\beta_{(C)}$ are the result of the impact of surface heterogeneity on backscatter even when aggregated to 9 km resolution which apparently affects its sensitivity towards soil moisture. Hence, these 24 different $\beta_{(C)}$ for each orbit for σ°_{VH} (Table 4) and 24 different $\beta_{(C)}$ for each orbit for σ°_{VV} (Table 5) were used in the baseline algorithm as discussed in Section 4.3 to downscale SMAP SSMI to a medium resolution of 50 m for σ°_{VV} and σ°_{VH} .



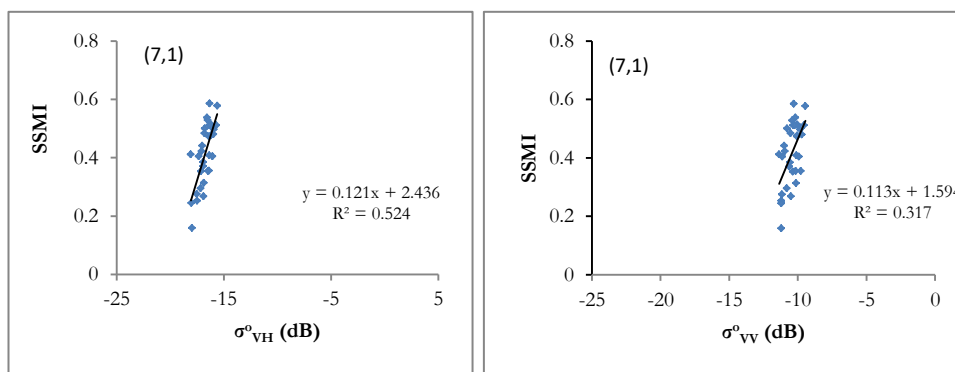
a) Orbit 15



b) Orbit 37



a) Orbit 88



b) Orbit 139

Figure 12: Figure showing the correlation between surface soil moisture index and backscattering coefficient for selected pixel for different orbital passes.

Table 4: Soil moisture sensitive parameters ($\alpha_{(C)}$ and $\beta_{(C)}$) and R^2 for all 24 pixels and 4 orbital passes for σ_{VH} . The bold values show the minimum and the maximum range of $\beta_{(C)}$ and R^2 .

S No	Pixel	Orbit_15			Orbit_37			Orbit_88			Orbit_139		
		$\alpha_{(C)}$	$\beta_{(C)}$	R^2	$\alpha_{(C)}$	$\beta_{(C)}$	R^2	$\alpha_{(C)}$	$\beta_{(C)}$	R^2	$\alpha_{(C)}$	$\beta_{(C)}$	R^2
1	(0,0)	2.504	0.121	0.514	2.233	0.099	0.307	1.896	0.082	0.325	2.281	0.101	0.245
2	(1,0)	2.177	0.106	0.584	1.733	0.075	0.293	1.446	0.059	0.324	1.854	0.081	0.280
3	(2,0)	2.200	0.105	0.607	1.910	0.086	0.388	1.492	0.060	0.326	2.034	0.089	0.357
4	(3,0)	2.010	0.093	0.530	1.785	0.079	0.347	1.406	0.054	0.300	1.806	0.076	0.314
5	(4,0)	2.075	0.100	0.578	2.078	0.099	0.419	1.508	0.061	0.366	1.957	0.087	0.362
6	(5,0)	1.849	0.083	0.544	1.789	0.078	0.401	1.327	0.049	0.351	1.688	0.069	0.369
7	(6,0)	1.883	0.085	0.537	1.817	0.080	0.424	1.366	0.051	0.374	1.622	0.066	0.348
8	(7,0)	1.910	0.088	0.563	1.856	0.083	0.522	1.404	0.054	0.414	1.604	0.066	0.369
9	(0,1)	2.221	0.102	0.546	2.146	0.094	0.380	1.808	0.075	0.402	2.175	0.094	0.310
10	(1,1)	2.109	0.098	0.564	2.085	0.094	0.409	1.555	0.063	0.375	1.941	0.083	0.324
11	(2,1)	2.308	0.112	0.442	2.200	0.103	0.326	1.670	0.070	0.341	2.042	0.089	0.291
12	(3,1)	2.059	0.096	0.442	2.200	0.104	0.338	1.629	0.066	0.330	1.855	0.078	0.263
13	(4,1)	1.937	0.091	0.506	2.066	0.097	0.400	1.555	0.063	0.391	1.801	0.077	0.338
14	(5,1)	2.011	0.101	0.553	2.172	0.108	0.488	1.619	0.072	0.413	2.008	0.095	0.414
15	(6,1)	2.051	0.103	0.621	2.175	0.108	0.573	1.620	0.071	0.447	1.992	0.093	0.454
16	(7,1)	2.444	0.128	0.644	2.526	0.131	0.642	1.875	0.086	0.451	2.436	0.121	0.524
17	(0,2)	2.111	0.098	0.559	1.842	0.078	0.345	1.685	0.069	0.397	2.081	0.090	0.353
18	(1,2)	2.180	0.104	0.516	2.202	0.103	0.398	1.748	0.075	0.413	2.105	0.092	0.319
19	(2,2)	2.366	0.110	0.580	2.476	0.115	0.459	1.838	0.075	0.409	2.079	0.086	0.301
20	(3,2)	2.030	0.092	0.487	2.142	0.098	0.373	1.605	0.063	0.370	1.749	0.070	0.277
21	(4,2)	1.660	0.072	0.425	1.566	0.065	0.274	1.336	0.049	0.352	1.525	0.059	0.290
22	(5,2)	1.653	0.073	0.575	1.491	0.073	0.460	1.224	0.044	0.400	1.550	0.063	0.388
23	(6,2)	1.457	0.062	0.535	1.491	0.063	0.503	1.150	0.040	0.398	1.441	0.057	0.428
24	(7,2)	1.335	0.054	0.425	1.333	0.053	0.422	1.078	0.035	0.352	1.301	0.049	0.373

Table 5: Soil moisture sensitive parameters ($\alpha_{(C)}$ and $\beta_{(C)}$) and R^2 for all 24 pixels and 4 orbital passes for σ_{VV} . The bold values show the minimum and the maximum range of $\beta_{(C)}$ and R^2 .

S No	Pixel	Orbit_15			Orbit_37			Orbit_88			Orbit_139		
		$\alpha_{(C)}$	$\beta_{(C)}$	R^2	$\alpha_{(C)}$	$\beta_{(C)}$	R^2	$\alpha_{(C)}$	$\beta_{(C)}$	R^2	$\alpha_{(C)}$	$\beta_{(C)}$	R^2
1	(0,0)	1.060	0.055	0.179	1.472	0.086	0.213	1.542	0.091	0.317	1.272	0.064	0.110
2	(1,0)	1.024	0.055	0.212	1.368	0.081	0.231	1.419	0.086	0.362	1.110	0.055	0.108
3	(2,0)	1.039	0.057	0.234	1.458	0.092	0.332	1.339	0.080	0.345	1.297	0.071	0.192
4	(3,0)	0.879	0.043	0.172	1.271	0.076	0.282	1.207	0.069	0.303	1.139	0.059	0.157
5	(4,0)	0.961	0.053	0.234	1.319	0.082	0.351	1.277	0.077	0.378	1.168	0.066	0.185
6	(5,0)	0.896	0.042	0.226	1.111	0.057	0.296	1.299	0.072	0.414	1.039	0.049	0.148
7	(6,0)	0.904	0.043	0.225	1.062	0.054	0.275	1.340	0.076	0.437	0.950	0.043	0.121
8	(7,0)	0.950	0.047	0.239	1.023	0.051	0.277	1.358	0.077	0.443	0.943	0.043	0.122
9	(0,1)	0.958	0.044	0.157	1.310	0.069	0.192	1.487	0.083	0.372	1.145	0.052	0.097
10	(1,1)	0.937	0.045	0.167	1.359	0.077	0.255	1.417	0.083	0.402	1.114	0.053	0.109
11	(2,1)	0.991	0.052	0.162	1.425	0.088	0.226	1.442	0.088	0.345	1.193	0.062	0.118
12	(3,1)	0.865	0.039	0.116	1.272	0.073	0.208	1.424	0.084	0.329	1.079	0.052	0.092
13	(4,1)	0.911	0.045	0.175	1.241	0.071	0.269	1.423	0.086	0.425	1.212	0.066	0.170

14	(5,1)	1.028	0.062	0.267	1.318	0.092	0.365	1.318	0.086	0.428	1.254	0.082	0.250
15	(6,1)	1.089	0.068	0.330	1.255	0.082	0.337	1.334	0.087	0.460	1.232	0.078	0.250
16	(7,1)	1.392	0.098	0.434	1.449	0.103	0.401	1.579	0.108	0.476	1.594	0.113	0.316
17	(0,2)	1.010	0.049	0.203	1.309	0.072	0.210	1.503	0.086	0.431	1.270	0.063	0.144
18	(1,2)	0.951	0.045	0.143	1.401	0.083	0.232	1.479	0.089	0.387	1.235	0.063	0.115
19	(2,2)	1.032	0.049	0.189	1.310	0.070	0.214	1.628	0.096	0.414	1.165	0.053	0.099
20	(3,2)	0.871	0.038	0.129	1.140	0.058	0.176	1.381	0.078	0.361	1.109	0.052	0.107
21	(4,2)	0.767	0.030	0.126	0.896	0.039	0.131	1.227	0.066	0.396	1.067	0.052	0.151
22	(5,2)	0.909	0.044	0.285	1.071	0.056	0.301	1.154	0.062	0.476	1.182	0.064	0.263
23	(6,2)	0.802	0.035	0.251	0.910	0.044	0.269	1.018	0.051	0.418	1.021	0.053	0.241
24	(7,2)	0.740	0.029	0.187	0.828	0.036	0.209	0.930	0.043	0.346	0.949	0.046	0.211

5.2. SMAP L4 SSMI vs RSMI

Relationships between the SMAP surface and root zone soil moisture indices were developed for each SMAP pixels. It is known that a non-linear relationship exists between the surface and root zone soil moisture (Dumedah et al., 2015). We have opted for a natural exponential function because compared to other statistical regressions, this gave the highest value of R^2 and good correlation for all 24 pixels. The mathematical formulation of the relationship developed is as shown in equation (9).

$$RSMI = a * e^{(b*SSMI)} \quad (9)$$

Where, RSMI is the root zone soil moisture index and SSMI is the surface soil moisture index and are unitless, a and b are the coefficients and e is a numerical constant.

For 24 SMAP pixels in the study area, 24 different relationships between surface and root zone soil moisture indices were developed. Figure 13 shows the highest value of R^2 i.e., 0.989 and the lowest value of R^2 i.e., 0.933 out of 24 statistical relationships developed between SMAP surface and root zone soil moisture indices. A good correlation between surface and root zone soil moisture index was obtained in all the pixels with very high R^2 values. This was an expected result as SMAP L4 soil moisture product is obtained from a modelled result where the catchment land surface model used for the assimilation process has a very strong coupling between root zone and surface soil moisture (Koster et al., 2000).

There are some outliers as seen in Figure 13 in pixel (2,2), these outliers can be assumed to signify that after a rainfall occurrence the top soil or the surface soil gets wet first and then it infiltrates to root zone and takes time to get wet. The minimum value of SSMI is seen to be fluctuating for different pixel. The reason behind the varying minimum SSMI can be explained by the fact that the rainfall in the study area is not uniform in time (Figure 2) which affects the moisture condition in the soil. This moisture condition for surface layer can also be affected by the type of soil, since our study area mainly consists of sandy soil which have lower soil moisture content and loamy soil which have higher soil moisture content. Whereas, the minimum value of RSMI seems to remain constant or above a certain value (i.e. ≈ 0.25) for all pixel which might be the influence of the ground water table.

Table 6 shows all 24 different coefficients and corresponding R^2 obtained from equation (9). In this table we can see that the value of the coefficients varies from 0.127 to 0.139 and coefficient b varies from 2.032 to 2.344. It can also be noted that value of b changes according to the correlation between surface and root zone soil moisture, for instance highly correlated pixel (0,0) with R^2 as 0.989 has the highest value of b (i.e. 2.344). Thus coefficient b can also be considered to be slightly sensitive towards the relationship between RSMI and SSMI but this assumption needs some more analysis.

The downscaled SMAP SSMI for σ_{VV} and σ_{VH} obtained from Section 5.1 were used with the coefficients in Table 6 in the relationship shown in equation (9) to get RSMI for σ_{VV} and σ_{VH} at a resolution of 50 m. These downscaled SSMI and RSMI were translated into volumetric surface soil moisture content and root zone soil moisture content as explained in equation (5) of Section 4.4.

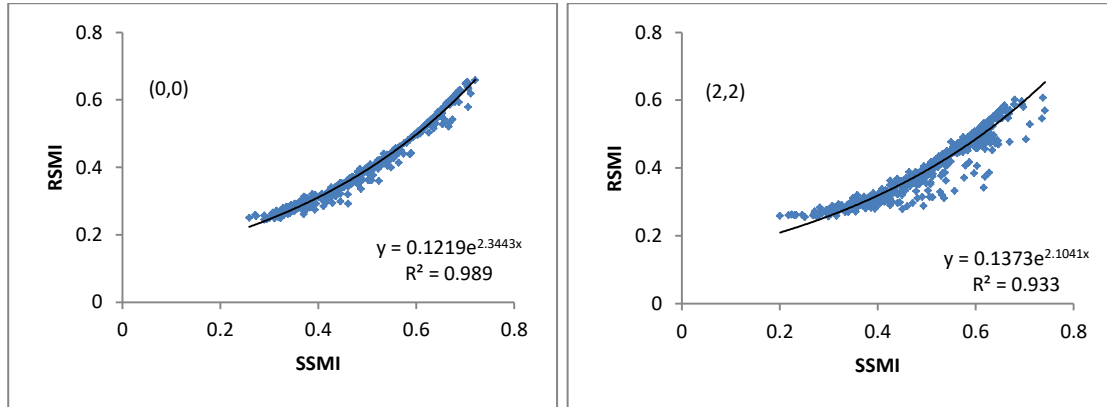


Figure 13: Scatter plot showing the agreement between SMAP surface and root zone soil moisture index, scatter plot for pixel (0,0) shows the highest and scatter plot for pixel (2,2) shows the lowest out of 24 pixels.

Table 6: The parameters (a and b) from equation (9) and R² obtained from the relationship developed between the SMAP SSMI and RSMI for all 24 pixels. The bold values show the minimum and the maximum range

S No	Pixel	a	b	R ²
1	(0,0)	0.122	2.344	0.989
2	(0,1)	0.127	2.230	0.987
3	(0,2)	0.154	2.026	0.961
4	(1,0)	0.130	2.196	0.975
5	(1,1)	0.128	2.240	0.980
6	(1,2)	0.125	2.294	0.983
7	(2,0)	0.129	2.210	0.975
8	(2,1)	0.127	2.258	0.981
9	(2,2)	0.137	2.104	0.933
10	(3,0)	0.131	2.185	0.971
11	(3,1)	0.128	2.238	0.978
12	(3,2)	0.127	2.260	0.980
13	(4,0)	0.133	2.140	0.962
14	(4,1)	0.132	2.162	0.967
15	(4,2)	0.132	2.168	0.966
16	(5,0)	0.134	2.118	0.954
17	(5,1)	0.138	2.050	0.950
18	(5,2)	0.139	2.041	0.944
19	(6,0)	0.137	2.065	0.952
20	(6,1)	0.139	2.032	0.942
21	(6,2)	0.139	2.034	0.937
22	(7,0)	0.137	2.074	0.953
23	(7,1)	0.138	2.309	0.954
24	(7,2)	0.136	2.090	0.949

6. VALIDATION

6.1. SMAP L4 surface soil moisture product

The SMAP L4 surface soil moisture (9 km) was validated against the in-situ surface soil moisture to analyse the accuracy of the coarse resolution SMAP product. For surface soil moisture out of 20 stations present in the study area which gave reading for top 5 cm, 17 stations were considered and 3 stations (ITCSM_06, ITCSM_11 and ITCSM_15) were discarded because of lots of missing data in those stations. A time series of the averaged SMAP surface soil moisture estimates over Twente region and the averaged in-situ measurements of top 5 cm of soil surface from all the 17 stations were plotted which can be seen in Figure 14. The mean value of averaged SMAP surface soil moisture is $0.215 \text{ m}^3 \text{ m}^{-3}$ whereas in-situ soil moisture is $0.291 \text{ m}^3 \text{ m}^{-3}$. The standard deviation of SMAP surface soil moisture is $0.036 \text{ m}^3 \text{ m}^{-3}$ and of the in-situ measurements is $0.094 \text{ m}^3 \text{ m}^{-3}$. These statistical variations show that the SMAP product underestimates the in-situ measurements and bias correction is required to be done to matchup the SMAP estimation with the in-situ measurements.

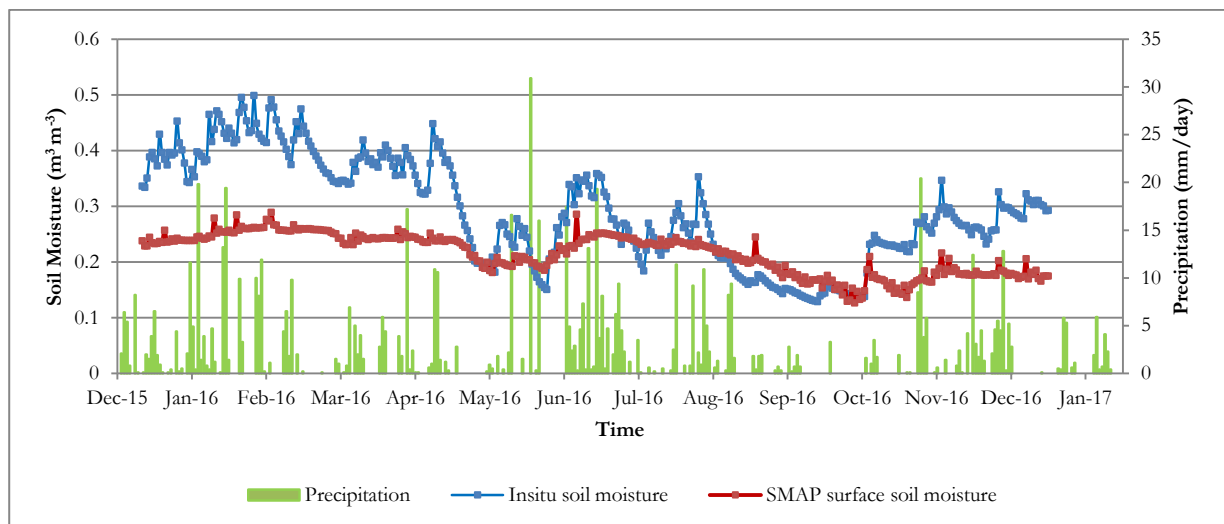


Figure 14: Time series showing the average retrieved coarse resolution SMAP surface soil moisture against the averaged in-situ soil moisture measurements for the study area and the rainfall data.

A good matchup was seen in the trend of bias corrected SMAP data (using the method explained in Section 4.5) and the in-situ measurements, as shown in Figure 15. We can see that a good correlation and a small bias between SMAP surface soil moisture and in-situ measurements from January till June exists, but this correlation seems to be absent during the month of July till October. Between July and October there is high vegetation in this study area. Therefore, this discrepancy is probably due to different agricultural fields with different types of vegetation in the study area but is not properly represented in the SMAP pixel. The Catchment land surface model used for SMAP L4 assimilation works in a fixed computational unit of 9 km but within a 9 km field in the study area different types of vegetation (crops, grass and forest) are seen, which can result in imperfect parameterization like evapotranspiration in the model, as different types of vegetation can affect the rate of evapotranspiration even within an area of few hectares. Similar result was seen in an study done by Zhang et al. (2017) where they analysed SMAP L4 soil moisture product for different terrain types in the United States and found that SMAP L4 soil moisture product shows a good agreement with in-situ measurements during winter but the agreement starts decreasing when the density of vegetation starts increasing in summer.

In spite of a similar trend of soil moisture variability, a bias still exists between SMAP and in-situ data during November and December. This variation can also be explained by imperfect model parameterization, as the model does not consider frozen soil or snow cover condition (SMAP Science Team, 2014). But when we compare with the air temperature data for the study area which can be seen in Appendix 1, the daily average temperature in the months of November and December occasionally reaches -5°C which can cause frozen soil condition and even be related to snow fall. This can lead to discrepancies between the model parameters and the actual field condition of the study area. Consequently, the ubRMSE and R^2 from the matchups gives $0.066 \text{ m}^3 \text{ m}^{-3}$ and 0.573 respectively which does not support the result obtained by Reichle et al., (2016) where SMAP L4 surface soil moisture was able to meet the targeted ubRMSE of $0.04 \text{ m}^3 \text{ m}^{-3}$.

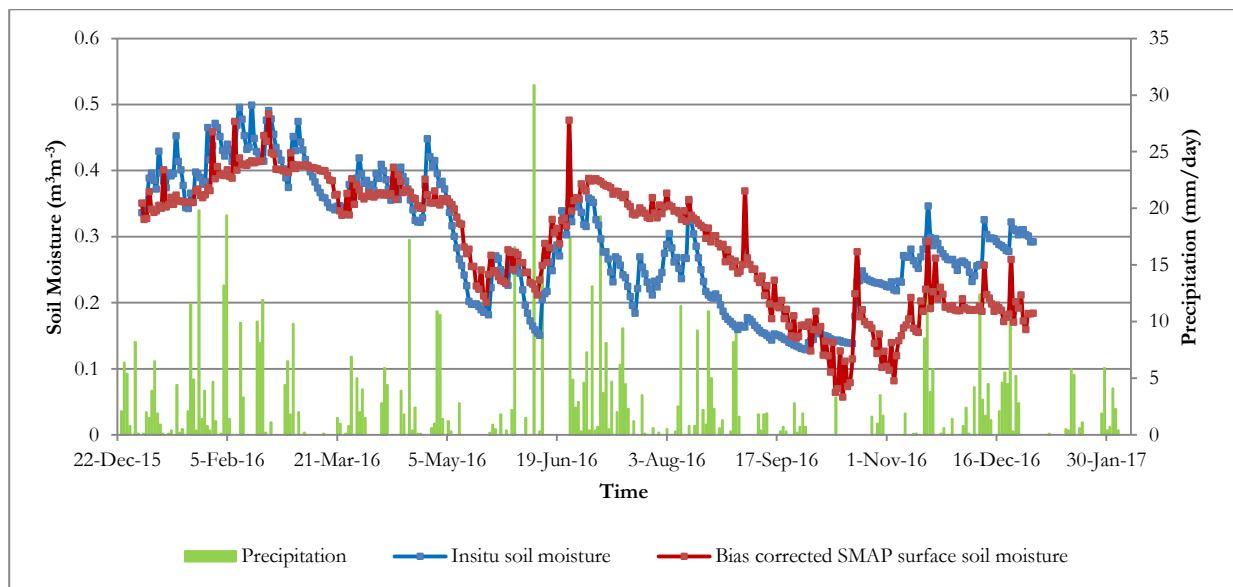


Figure 15: Time series showing the averaged retrieved coarse resolution SMAP surface soil moisture against the averaged in-situ soil moisture measurements and the rainfall data after the bias correction of SMAP data.

The SMAP surface soil moisture estimate from individual pixel was also compared with the data from the corresponding soil moisture monitoring stations. Out of the 24 SMAP pixels in the study area, 17 pixels contained soil moisture measurement stations. The 17 pixels with corresponding soil moisture monitoring stations can be seen in Table 7 which also shows the ubRMSE and R^2 calculated for the time series of 17 stations and the corresponding pixel value. Table shows the highest correlation with R^2 of 0.824 for the forest site (ITCSM_20) which signifies that the soil moisture variation of this site is well represented by the SMAP pixel (2,1). The lowest correlation is seen for station 07 and station 10 which lies next to crop field. Thus, it can be said that the temporal variation of crops (especially corn) in field scale is not well represented by the SMAP pixel, which can also be justified by the result seen for Station 01 and Station 07. Although both stations lie within the same SMAP pixel (7,0), Station 01 which is in a grassland shows higher value of R^2 than station 07 which lies next to cornfield.

Table 7: Error metrics (ubRMSE and R^2) for surface soil moisture retrieved from each SMAP pixel and the corresponding soil moisture monitoring stations in it. The bold values show the minimum and the maximum range.

Stations	Pixel	ubRMSE ($\text{m}^3 \text{ m}^{-3}$)	R^2
ITCSM_01	(7,0)	0.086	0.441
ITCSM_02	(6,0)	0.105	0.354
ITCSM_03	(5,0)	0.11	0.446

ITCSM_04	(7,1)	0.125	0.456
ITCSM_05	(4,1)	0.121	0.017
ITCSM_07	(7,0)	0.1	0.09
ITCSM_08	(5,2)	0.052	0.358
ITCSM_09	(6,2)	0.099	0.181
ITCSM_10	(4,2)	0.1	0.018
ITCSM_12	(3,2)	0.111	0.492
ITCSM_13	(1,2)	0.059	0.582
ITCSM_14	(0,2)	0.106	0.548
ITCSM_16	(3,0)	0.096	0.502
ITCSM_17	(3,0)	0.113	0.422
ITCSM_18	(1,0)	0.102	0.343
ITCSM_19	(0,0)	0.167	0.657
ITCSM_20	(2,1)	0.025	0.824
Mean		0.099	0.369

6.2. SMAP L4 root zone soil moisture product

The SMAP root zone soil moisture (9 km) was validated against the in-situ soil moisture data obtained from the available four stations. For root zone soil moisture only 6 out of 20 stations (ITCSM_06, ITCSM_10, ITCSM_11, ITCSM_14, ITCSM_15 and ITCSM_17) provided data for the depth of 80 cm out of which ITCSM_06 and ITCSM_11 were discarded because of lack of consistent data. Since the in-situ measurements provides data for only down to 80 cm depth and the SMAP root zone soil moisture refers to a layer down to 1 m depth, the difference had to be compensated for checking the reliability of the SMAP product with in-situ measurements.

The available soil moisture monitoring stations gives the measurements for the depth of 5 cm, 10 cm, 20 cm, 40 cm and 80 cm, weighted average of these measurements were calculated considering data for 80 cm depth to represent the moisture down to 1 m. The weighted average is done in such a way that data from each depth has its own contributing weightage (i.e. 7.5% for 5 cm, 7.5% for 10 cm, 15% for 20 cm, 30% for 40 cm and 40% for 80 cm depth). Since the four stations were not distributed over the whole study area, instead of averaging soil moisture retrieval to whole area only pixels consisting of these four stations were selected and averaged. These averaged measurements were compared with the weighted average of in-situ measurements which can also be seen in Appendix 2. The result shows a large bias in mean and standard deviation of the in-situ and SMAP data. The mean value of in-situ measurements is $0.407 \text{ m}^3 \text{ m}^{-3}$ whereas for SMAP data is $0.173 \text{ m}^3 \text{ m}^{-3}$ and similarly the standard deviation of in-situ is $0.046 \text{ m}^3 \text{ m}^{-3}$ and for SMAP is $0.026 \text{ m}^3 \text{ m}^{-3}$. These biases in mean and in standard deviation were removed by rescaling SMAP data to in-situ measurements as explained in Section 4.5.

The time series of bias corrected SMAP root zone soil moisture and in-situ measurements are shown in Figure 16. Figure shows that the data for the months of January till March are missing because inconsistency was seen in the in-situ measurements at different layers during these periods for which the data were discarded to reduce the bias within the measurements. Figure 16 shows that unlike surface soil moisture (Figure 15) there is a better correlation in the temporal distribution of soil moisture even during the month of July until October which is the period when high vegetation is seen in this study area. This result suggests that the SMAP root zone soil moisture seems to be less affected by the temporal variation of vegetation. Bias is seen in the time series of SMAP and in-situ data for the month of November and

December which perhaps can be the effect of groundwater table which is increased in this period but is not properly implemented in the SMAP model. The calculated bias corrected ubRMSE and R^2 is $0.036 \text{ m}^3 \text{ m}^{-3}$ and 0.360 respectively which meets the SMAP requirement of $0.04 \text{ m}^3 \text{ m}^{-3}$. Regardless of better ubRMSE value, there exists an overall low R^2 and can be the result of limited datasets available for root zone soil moisture validation from few soil moisture monitoring stations (4 out of 20) in the Twente region.

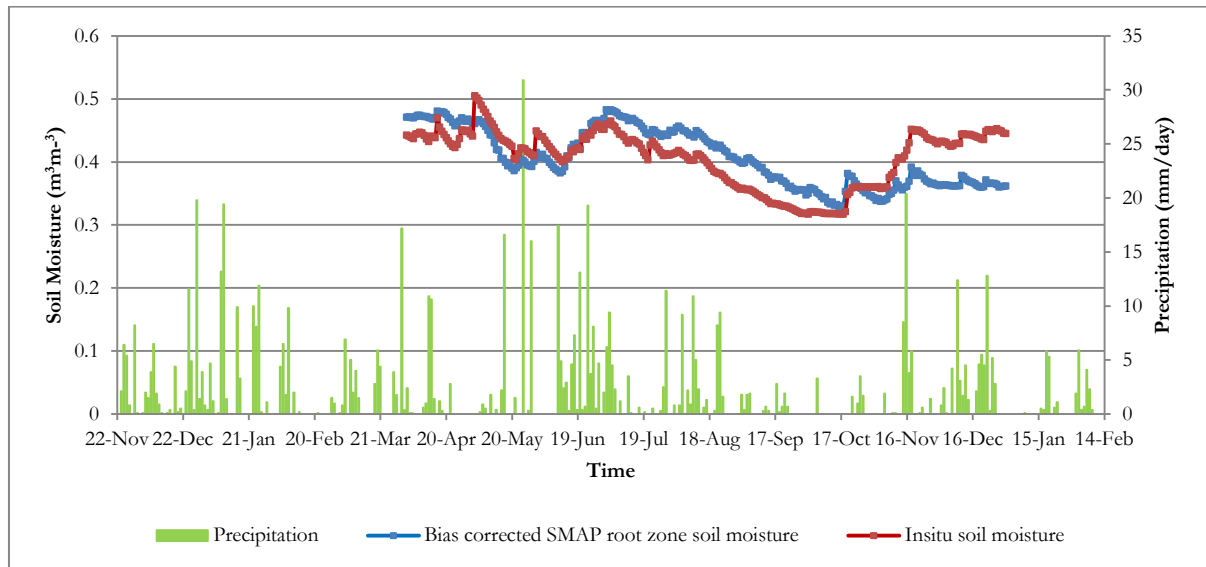


Figure 16: Time series showing the averaged retrieved coarse resolution SMAP root zone soil moisture against the averaged in-situ soil moisture measurements and the rainfall data after the bias correction of SMAP data.

The weighted average measurements for top 100 cm obtained from all the 4 stations were also individually compared with SMAP root zone soil moisture estimates from corresponding pixels. Table 8 shows the bias corrected ubRMSE and R^2 calculated from the time series of 4 stations and the corresponding pixel value. Station 17, pixel (3,0) shows highest value of R^2 as 0.603 and ubRMSE of $0.048 \text{ m}^3 \text{ m}^{-3}$ which signifies that the root zone soil moisture dynamics is well represented by this SMAP pixel. Whereas, station 10 shows the ubRMSE of $0.109 \text{ m}^3 \text{ m}^{-3}$ and R^2 of 0.033 and can be the result of different soil type, infiltration rate and groundwater depth on field scale which is not represented properly by the SMAP footprint.

Table 8: Error metrics (ubRMSE and R^2) for root zone soil moisture retrieved from each SMAP pixel and the corresponding field measurement stations in it. The bold values show the minimum and the maximum range.

Stations	Pixels	ubRMSE ($\text{m}^3 \text{ m}^{-3}$)	R^2
ITCSM_10	(4,2)	0.109	0.033
ITCSM_14	(0,2)	0.043	0.411
ITCSM_15	(3,1)	0.034	0.202
ITCSM_17	(3,0)	0.048	0.603
Mean		0.059	0.312

6.3. Downscaled surface soil moisture

Downscaled surface soil moisture (50 m) retrieved from both $\sigma^{\circ}_{\text{VH}}$ and $\sigma^{\circ}_{\text{VV}}$ were separately compared with the in-situ soil moisture measurements to see which polarization is more suitable for soil moisture estimation. A time series of average of all the data obtained from 17 stations and the bias corrected downscaled surface soil moisture data (for $\sigma^{\circ}_{\text{VH}}$ and $\sigma^{\circ}_{\text{VV}}$) averaged over the study area was created which is shown in Figure 17 and Figure 18. In these figures when downscaled surface soil moisture is compared with

in-situ measurements, correlation in the time series is seen to be decreasing during the month of July till October and some bias is seen for the month of November and December for both σ_{VH} and σ_{VV} . As explained in Section 6.1 (Figure 15), similar result is seen in the time series of SMAP surface soil moisture. This suggests that the accuracy performance of downscaled product depends upon the quality of the input data, which was also discussed in a study done by Peng et al., (2016).

The ubRMSE and R^2 was calculated as $0.068 \text{ m}^3 \text{ m}^{-3}$ and 0.533 respectively for σ_{VH} and $0.062 \text{ m}^3 \text{ m}^{-3}$ and 0.593 respectively for σ_{VV} . Thus, it can be seen that the downscaled surface soil moisture product obtained from σ_{VV} is found to be better when compared to soil moisture obtained from σ_{VH} . This result also supports the study by Piles et al., (2009) and Bousbih et al., (2017) where they have found that VV has high potential in estimation of soil moisture when compared to VH. The downscaled surface soil moisture using σ_{VV} also showed an improvement in the accuracy when compared to the original SMAP product by improving the ubRMSE from $0.066 \text{ m}^3 \text{ m}^{-3}$ to $0.062 \text{ m}^3 \text{ m}^{-3}$ and R^2 from 0.573 to 0.593. This results supports the claim in previous studies (Piles et al., 2009 and Das et al., 2011) where airborne data sets were combined with synthetic data sets in a SMAP algorithm and a final product was retrieved with an increased accuracy. This indicates that the Sentinel-1 SAR data not only downscale SMAP, but also adds sensitivity to soil moisture.

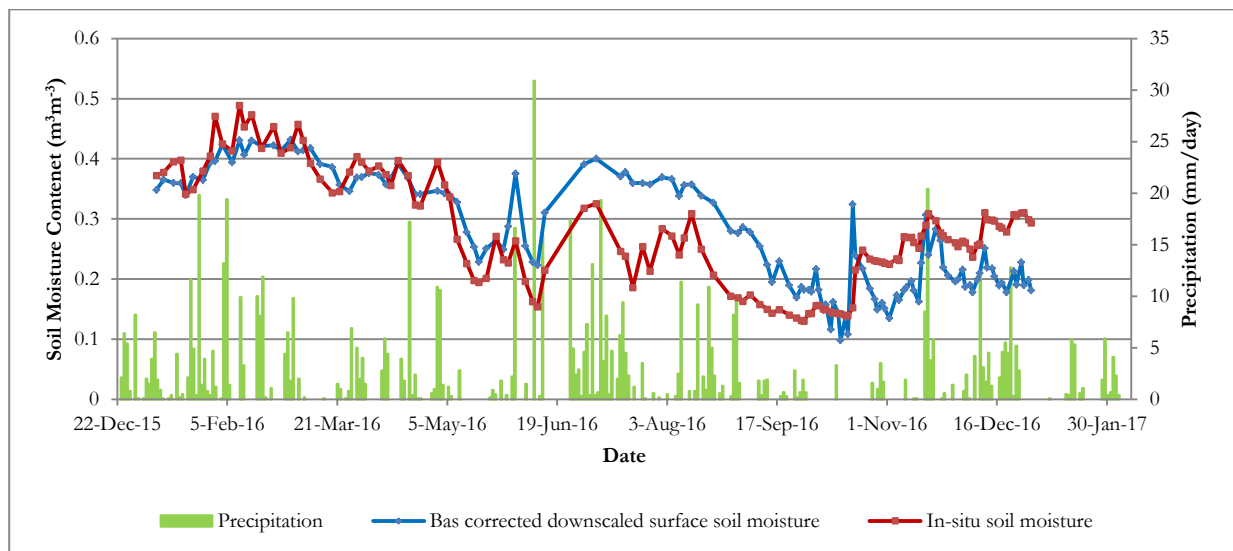


Figure 17: Time series showing the averaged retrieved downscaled SMAP surface soil moisture for σ_{VH} against the averaged in-situ soil moisture measurements and the rainfall data after the bias correction of SMAP data.

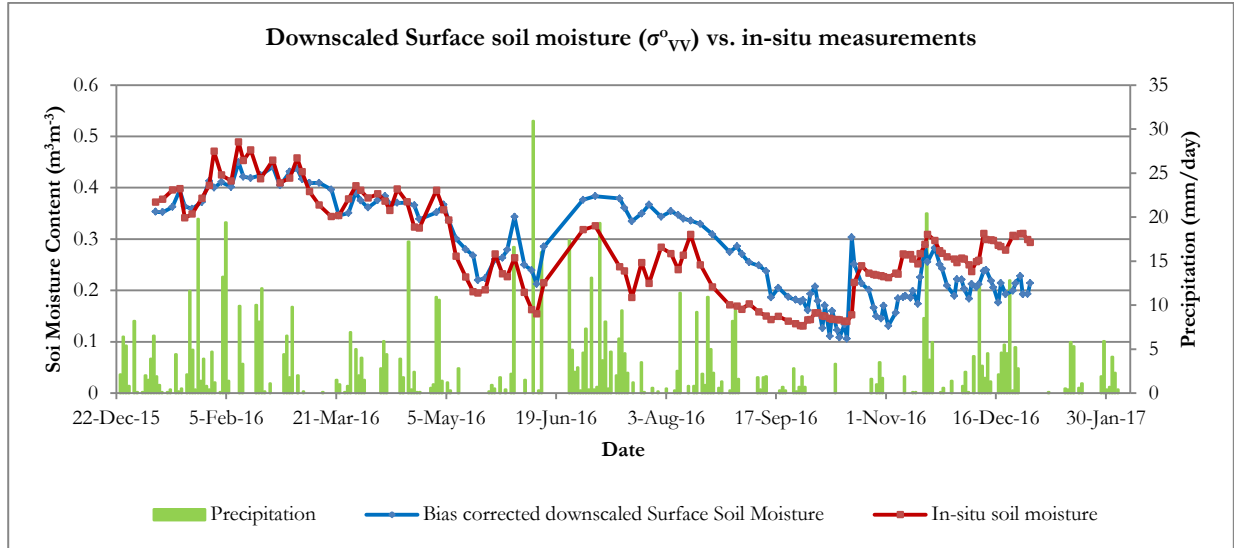


Figure 18: Time series showing the averaged retrieved downscaled SMAP surface soil moisture for σ^{0}_{VV} against the averaged in-situ soil moisture measurements and the rainfall data after the bias correction of SMAP data.

The data from individual soil moisture measurement stations and downscaled soil moisture data within a 5×5 grid cell of 50 m resolutions consisting of the corresponding soil moisture stations were compared. Table 9 shows the ubRMSE and R^2 for the data obtained from 16 stations and their corresponding average soil moisture data of 5×5 grid cells for σ^{0}_{VH} and σ^{0}_{VV} . We could see an increment in both ubRMSE and R^2 in soil moisture for σ^{0}_{VV} with individual stations (e.g. ITCSM_02, ITCSM_12, ITCSM_18) when compared to the R^2 of individual stations for SMAP pixel before downscaling (Table 7). Some stations (e.g. ITCSM_03, ITCSM_10, ITCSM_17 etc.) did not show significant improvement whereas, some stations even showed reduced accuracy. For instance we can see that for station 04 R^2 is 0.401 and ubRMSE is $0.134 \text{ m}^3 \text{ m}^{-3}$. This reduced ubRMSE can be argued to be the result of high land surface heterogeneity in the area of this station consisting of a mixture of cropland, residential and even forest area which might have interfered with the backscatter response towards soil moisture. As explained in previous studies (Piles et al., 2009 and Das et al., 2011) the assumption of $\beta_{(C)}$ as a homogeneous parameter for a radiometer footprint is one of the main reason to introduce error specially when the area is heterogeneous like the Twente region.

Table 9: Error metrics (ubRMSE and R^2) for individual field measurement stations and its corresponding downscaled surface soil moisture data for σ^{0}_{VH} averaged to 5×5 grid cells around the stations.

Stations	σ^{0}_{VH}		σ^{0}_{VV}	
	ubRMSE ($\text{m}^3 \text{ m}^{-3}$)	R^2	ubRMSE ($\text{m}^3 \text{ m}^{-3}$)	R^2
ITCSM_01	0.097	0.552	0.102	0.504
ITCSM_02	0.111	0.185	0.09	0.371
ITCSM_03	0.115	0.294	0.096	0.443
ITCSM_04	0.147	0.312	0.134	0.401
ITCSM_05	0.132	0.033	0.136	0.059
ITCSM_07	0.098	0.087	0.097	0.091
ITCSM_08	0.058	0.018	0.054	0.252
ITCSM_09	0.103	0.139	0.09	0.207
ITCSM_10	0.086	0.024	0.089	0.016
ITCSM_12	0.105	0.520	0.099	0.566
ITCSM_13	0.068	0.418	0.058	0.542

ITCSM_14	0.130	0.401	0.127	0.421
ITCSM_16	0.086	0.483	0.084	0.506
ITCSM_17	0.124	0.283	0.118	0.338
ITCSM_18	0.119	0.210	0.093	0.449
ITCSM_19	0.203	0.467	0.178	0.573
Mean	0.111	0.277	0.103	0.359

The bold values indicate the improvement in terms of both ubRMSE and R² for downscaled surface soil moisture.

6.4. Downscaled root zone soil moisture

The downscaled root zone soil moisture (50 m) from both σ_{VH} and σ_{VV} were separately validated against the in-situ soil moisture data obtained from the available four stations. As discussed earlier only four stations were available for the validation process which were not distributed over the whole study area so for each station a set of 5×5 pixels around those stations were selected and averaged. This average retrieved root zone soil moisture for σ_{VH} and σ_{VV} were compared separately with the weighted averages of root zone soil moisture measurements averaged for the 4 stations which is shown in Figure 19 and Figure 20 respectively. From this time series, the ubRMSE obtained was 0.051 m³ m⁻³ and R² of 0.184 for σ_{VH} and ubRMSE calculated 0.047 m³ m⁻³ and 0.266 for σ_{VV} . This result shows that σ_{VV} gives the relatively better estimates of soil moisture content for root zone.

Figure 19 and Figure 20 shows that the bias seen during the month of November and December also exists in the time series of downscaled root zone soil moisture and in-situ measurements. It can be seen that the downscaled root zone soil moisture shows some degradation in the accuracy assessment based on ubRMSE and R² when compared to the accuracy assessment of SMAP root zone soil moisture (Section 6.1). Although the relationship between SMAP surface and root zone soil moisture showed a very strong correlation, this relationship was developed for a 9 km grid cell and might not be beneficial in downscaling root zone soil moisture. In this study a higher resolution (250 m) soil physical properties data obtained from BOFEK2012 were used in downscaled root zone soil moisture. But when these downscaled soil moisture products were compared to the SMAP L4 soil moisture product downscaled root zone soil moisture showed a bias of 0.02 m³ m⁻³ which was not seen for downscaled surface soil moisture as seen in Appendix 3. This shows that the model parameters used in SMAP assimilation process at 9 km does not fit for the soil moisture condition at finer resolution. Thus, the relationship between SMAP surface and root zone soil moisture obtained at coarse resolution may not be same for finer resolution and is not beneficial to downscale root zone soil moisture.

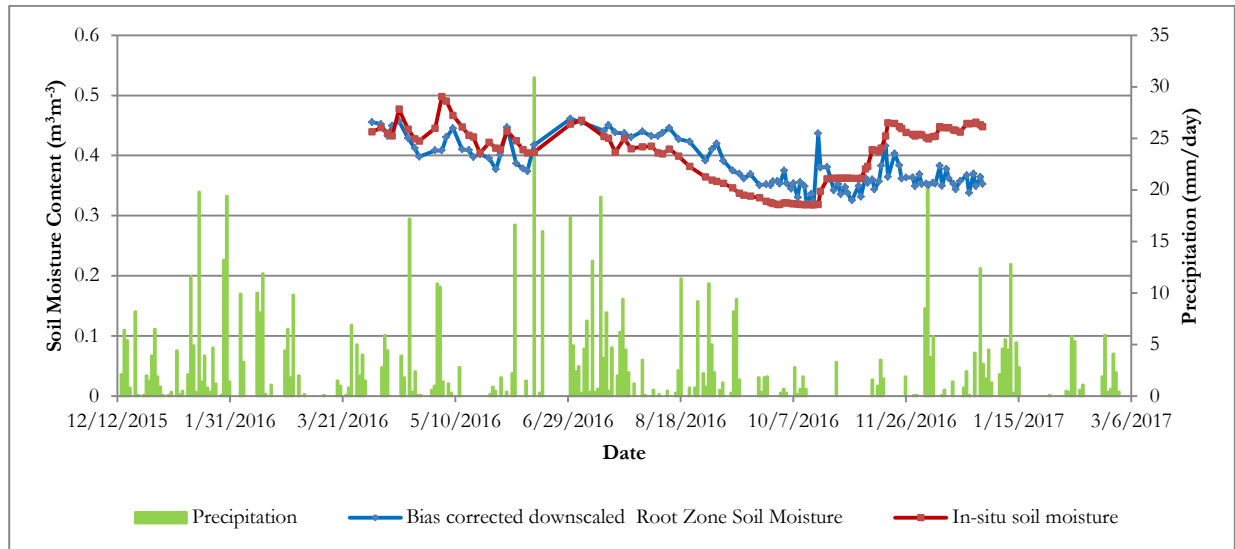


Figure 19: Time series showing the averaged downscaled SMAP root zone soil moisture for σ_{VH} against the averaged in-situ soil moisture measurements and the rainfall data after the bias correction of SMAP data.

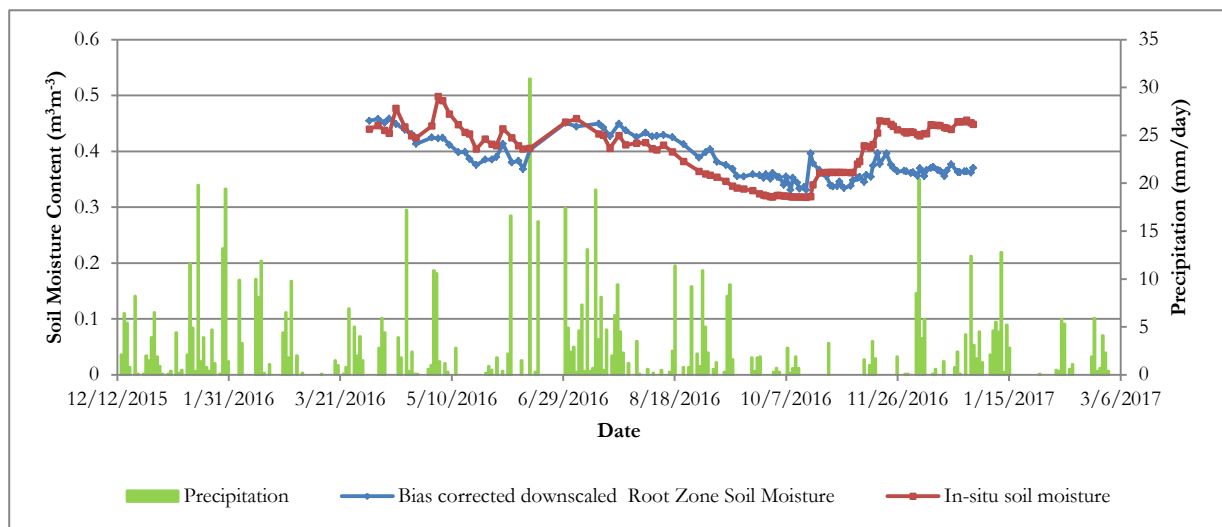


Figure 20: Time series showing the averaged downscaled SMAP root zone soil moisture for σ_{VV} against the averaged in-situ soil moisture measurements and the rainfall data after the bias correction of SMAP data.

The weighted averaged measurements for top 100 cm obtained from all the 4 stations were also individually compared with the corresponding average soil moisture data of 5×5 grid cell of 50 m resolutions for σ_{VH} and σ_{VV} . Table 10 shows ubRMSE and R^2 for the time series of 4 stations and the corresponding 5×5 pixel value. SMAP pixel at 9 km resolution which was assumed to have a better representation of root zone soil moisture dynamics in Section 6.2 showed an improvement in downscaled product as well. As seen in Table 10, R^2 and ubRMSE of downscaled root zone soil moisture (for σ_{VV}) increases for station 17 whereas decreases for other stations. Therefore improper representation of seasonal processes in the SMAP root zone soil moisture results in the degradation of downscaled root zone soil moisture.

Table 10: Error metrics for weighted average of field measurements from individual station and its corresponding downscaled surface soil moisture data for $\sigma^{\circ_{\text{VH}}}$ and $\sigma^{\circ_{\text{VV}}}$ which is the averaged data of 5×5 grid cells around the stations.

Stations	$\sigma^{\circ_{\text{VH}}}$		$\sigma^{\circ_{\text{VV}}}$	
	ubRMSE ($\text{m}^3 \text{m}^{-3}$)	R^2	ubRMSE ($\text{m}^3 \text{m}^{-3}$)	R^2
ITCSM_10	0.101	0.001	0.110	0.016
ITCSM_14	0.054	0.149	0.019	0.158
ITCSM_15	0.040	0.038	0.036	0.111
ITCSM_17	0.041	0.518	0.013	0.613
Mean	0.059	0.177	0.044	0.225

The bold values indicate the improvement in terms of both ubRMSE and R^2 for downscaled root zone soil moisture.

7. DOWNSCALING RESULTS

7.1. Downscaled surface soil moisture

As explained in Section 5.2, $\beta_{(C)}$ obtained from the relationship between SSMI and $\sigma^{\circ_{VH}}$ and $\sigma^{\circ_{VV}}$ were used to downscale SMAP SSMI which was further translated to volumetric surface soil moisture content and its validation with in-situ measurements is presented in Chapter 6.

Figure 21 shows the time series of downscaled surface soil moisture retrieval for $\sigma^{\circ_{VV}}$. When compared with the field measurements soil moisture retrieved with $\sigma^{\circ_{VV}}$ showed a better correlation as compared to $\sigma^{\circ_{VH}}$ as discussed in Chapter 6. The series of maps shown in Figure 21 show the temporal and the spatial variability of soil moisture content within the study area. In these maps, the grey colour shows the masked out urban and forest areas. The variation of spatial soil moisture distribution according to the land surface heterogeneity like the cultivated land and grassland can also be seen in these maps where the grassland shows higher soil moisture content than the agricultural field.

A temporal variation of soil moisture in the year 2016 is seen with a good agreement with rainfall. Moderate wet soil moisture condition in May seems to increase resulting in extreme wet condition in July, probably due to uniform rainfall occurrences throughout the month of June and July (Figure 2). For instance, the snapshots of 2016/06/14 and 2016/06/30 show the difference in temporal variation of soil moisture in presence of rainfall. Even the occurrence of less rainfall can be related to the snapshots of 2016/10/15 and 2016/11/02 which shows a very dried condition with soil moisture ($< 0.08 \text{ m}^3 \text{ m}^{-3}$). Thus, the SMAP baseline algorithm used to downscale SMAP surface soil moisture using Sentinel-1 SAR is successful in retrieving spatial and temporal variation of surface soil moisture at fine resolution (50 m).

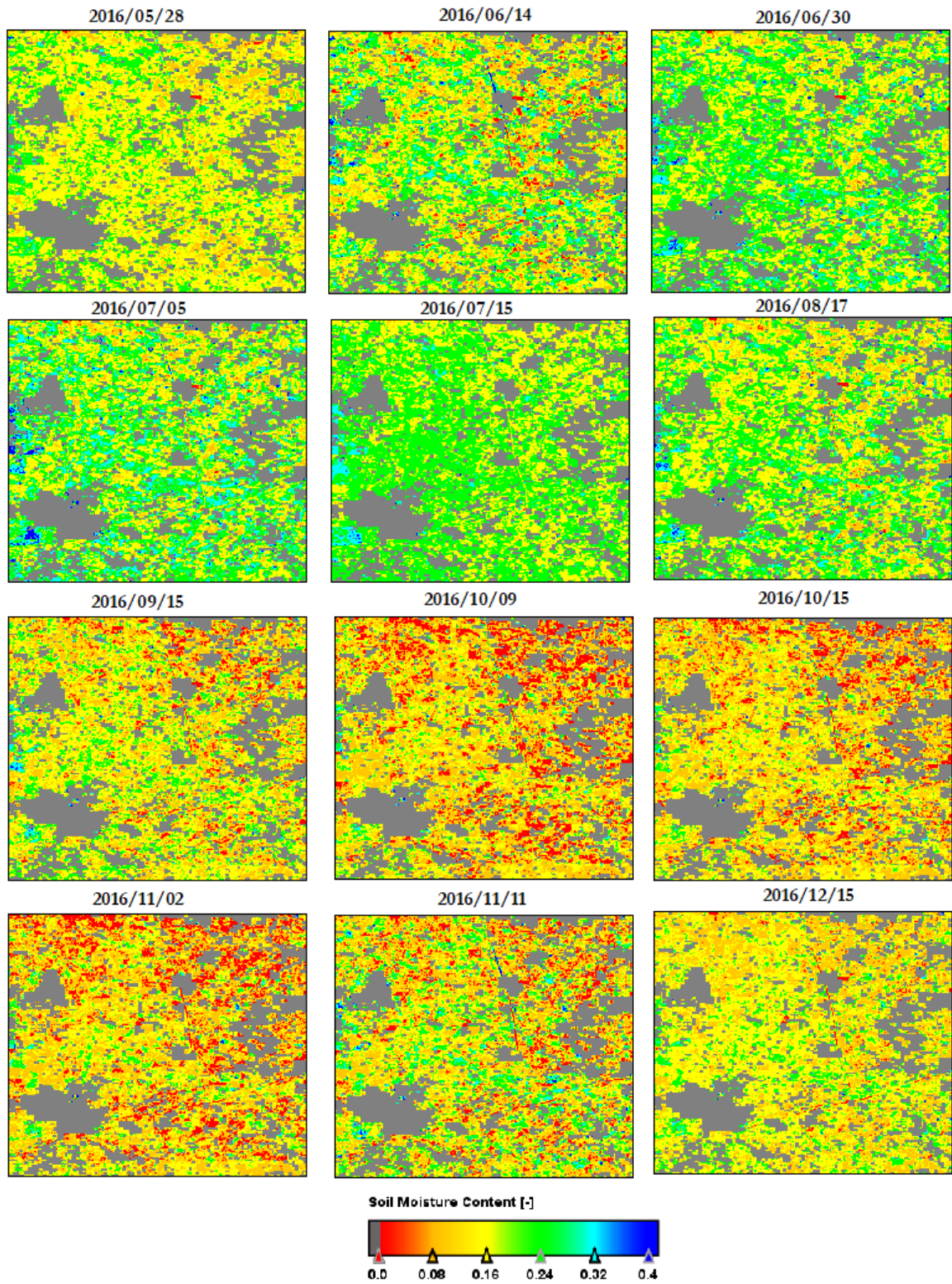


Figure 21: Series of surface soil moisture map downscaled to a resolution of 50 m obtained from combining SMAP L4 surface soil moisture and Sentinel-1 SAR backscattering coefficient.

7.2. Downscaled root zone soil moisture

The downscaled surface soil moisture was used in the relationship obtained between SMAP root zone and surface soil moisture index as explained in Section 5.2 to retrieve the root zone soil moisture at a finer resolution of 50 m. Since, surface soil moisture for $\sigma^{\circ_{VH}}$ and $\sigma^{\circ_{VV}}$ were used, root zone soil moisture was also retrieved for $\sigma^{\circ_{VH}}$ and $\sigma^{\circ_{VV}}$ at 50 m resolution.

Figure 22 shows the series of downscaled root zone soil moisture retrieval for $\sigma^{\circ_{VV}}$. When compared with the field measurements soil moisture retrieved with $\sigma^{\circ_{VV}}$ showed a better correlation as compared to $\sigma^{\circ_{VH}}$ as discussed in Chapter 6. Although the downscaled root zone soil moisture estimates showed some degradation in the accuracy assessment but it still shows some variation in spatial soil moisture distribution which can be seen in Figure 22. The grey colour shows the masked out urban and forest areas.

In the Figure series of maps can be seen which shows the temporal variation of soil moisture for the year 2016 where a moderate dry May to moderate wet July is seen, which again dries from October till December. But this is not the case in reality as the ground water depth increases during these periods (November and December). Thus, it can be said that the downscaling approach used in the retrieval of downscaled root zone soil moisture in this study does not represent the dynamics of soil moisture variation in field scale.

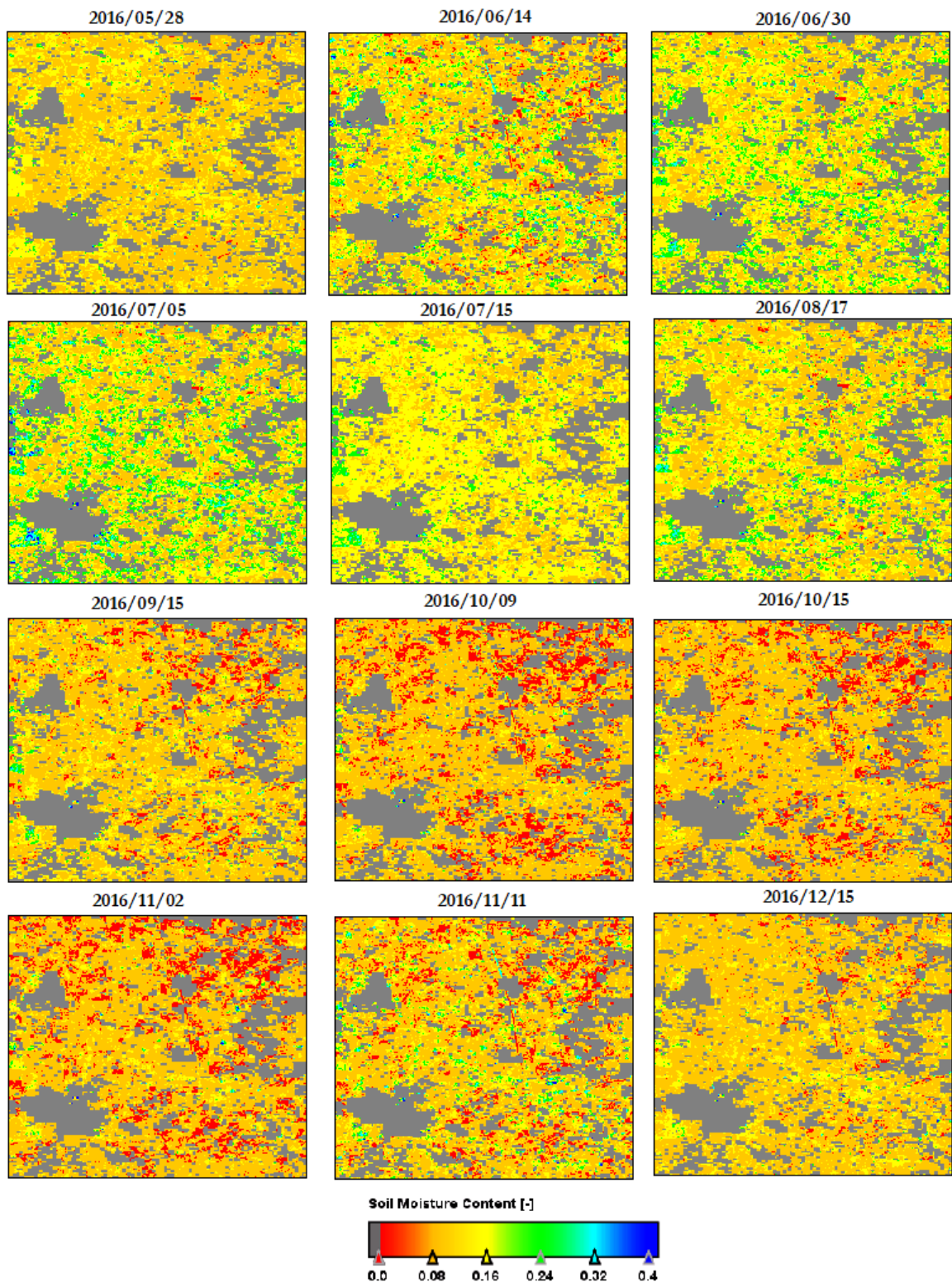


Figure 22: Series of root zone soil moisture map downscaled to a resolution of 50 m obtained from the relationship deduced between SMAP L4 surface and root zone soil moisture product.

8. DISCUSSION

The baseline algorithm used in downscaling surface soil moisture is dependent on the parameters describing the backscatter sensitivity towards soil moisture, which is obtained from the linear regression between radar backscatter and SMAP L4 surface soil moisture product. The active backscatter depends strongly on land surface variability in space and in time which can affect its sensitivity towards soil moisture. The vegetation morphology and vegetation water content helps in determining whether the backscatter is from ground surface or from the vegetation canopy itself (Bindlish & Barros, 2001 and Ferrazzoli et al., 1997). The Twente region being a heterogeneous area has different vegetation types especially grass, corn and forest. Thus, in this section we discuss the vegetation-related uncertainties related to Sentinel-1 SAR backscatter data retrieval.

Vegetation effect

To see the effect of vegetation cover on the active backscatter, an analysis was carried out to compare the backscatter from single grassland, forest and cornfield patches. The data were plotted against time which can be seen in Figure 23. In the figure, it can be seen that the backscatter from forest is high and remains almost constant over time whereas the backscatter received from grassland is relatively low and show small variations, it is almost constant over time. A large variation over time is seen in the backscatter obtained from cornfield.

For corn field, Figure 23 shows that the period of January to March shows a slight increased backscatter which can be the result of wet bare soil condition during these periods. In April and May we can see reduced backscatter with a very high variation over time which can be the result of the human activities like ploughing and sowing. Furthermore, sometimes the agricultural field is flooded with excess water that acts as smooth surface reducing the radar backscatter. For the months of June to September, cornfield shows high backscatter due to the vegetation canopy that remains constant over this period, unlike the observation during the months of November and December, when there is no corn on the fields and generally bare soil conditions are present. This is seen because of the dense and fast growing corn observed in Twente region, which has a strong effect on the backscatter and may hide the signal from the soil moisture during the period of June till September. Overall the radar backscatter shows less sensitivity towards soil moisture variation during the period of high vegetation and shows high sensitivity towards soil moisture in bare soil condition in winter. Thus, this change in sensitivity due to seasonal variation needs to be considered in future studies related to soil moisture estimation from radar data.

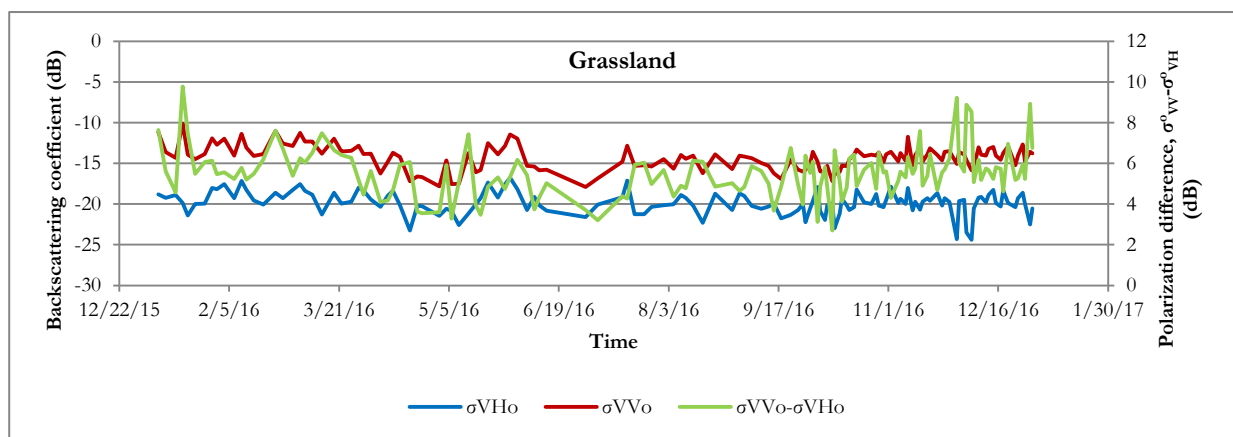




Figure 23: A time series showing the response of σ_{VH_0} , σ_{VV_0} and $\sigma_{VH_0} - \sigma_{VV_0}$ for different land cover types (Grassland, Corn field and Forest).

Effect of seasonal variation

To analyse the effect of the seasonal variations (summer and winter) on the soil moisture retrieval we compared the time series of SMAP soil moisture and downscaled soil moisture for summer and the winter season. The time series of SMAP surface soil moisture compared with in-situ measurements (Section 6.1) were separated for summer (From June till September) and winter (from January till May and November and December). An improved result was obtained when SMAP surface soil moisture was compared to in-situ measurements for summer and winter with R^2 obtained as 0.741 for winter and 0.810 for summer. Both summer and winter period showed a better correlation between SMAP surface soil moisture and in-situ soil moisture compared to the result obtained for the entire year (i.e. $R^2 = 0.573$). Figure 24 shows the scatter plot of SMAP surface soil moisture and downscaled surface soil moisture with in-situ soil measurements to illustrate their agreements for summer and winter seasons.

When the downscaled surface soil moisture was compared with in-situ measurements for different seasons, R^2 was found to be 0.773 for the winter and 0.783 for the summer. As expected, this result shows significant improvement when compared to that of entire year (i.e. $R^2 = 0.593$). The result also shows that the value of R^2 for downscaled surface soil moisture is slightly improved in winter when there is bare soil condition but slightly decreased in summer when there is vegetation on field as compared to SMAP surface soil moisture. As discussed earlier, this improved result signifies that the Sentinel-1 SAR backscatter is more sensitive towards soil moisture when there is no vegetation and retrieved soil moisture has better agreement with in-situ measurements. The degradation seen in summer season can be argued to be the effect of vegetation. Thus, more improved result can be expected if the parameter $\beta_{(C)}$, defining the backscatter sensitivity to soil moisture could be considered for the spatial and temporal variation of land surface

heterogeneity. Unlike the surface soil moisture, downscaled root zone soil moisture showed degradation during both summer and winter which can be seen in Appendix 4. The degradation in R^2 might be because of the limited field measurements available for validation. Furthermore, in the Twente region presence of shallow groundwater table (i.e. < 1 m) is seen, which increases during winter and might not be well represented in the catchment land surface model which results in additional error while quantifying root zone soil moisture at field scale as R^2 decreases more in winter. Thus, it can be said that due to imperfect parameterization embedded in the catchment land surface model, the downscaling of SMAP root zone soil moisture at field scale is affected and the accuracy assessment of downscaled root zone soil moisture is restricted by limited field measurements available.

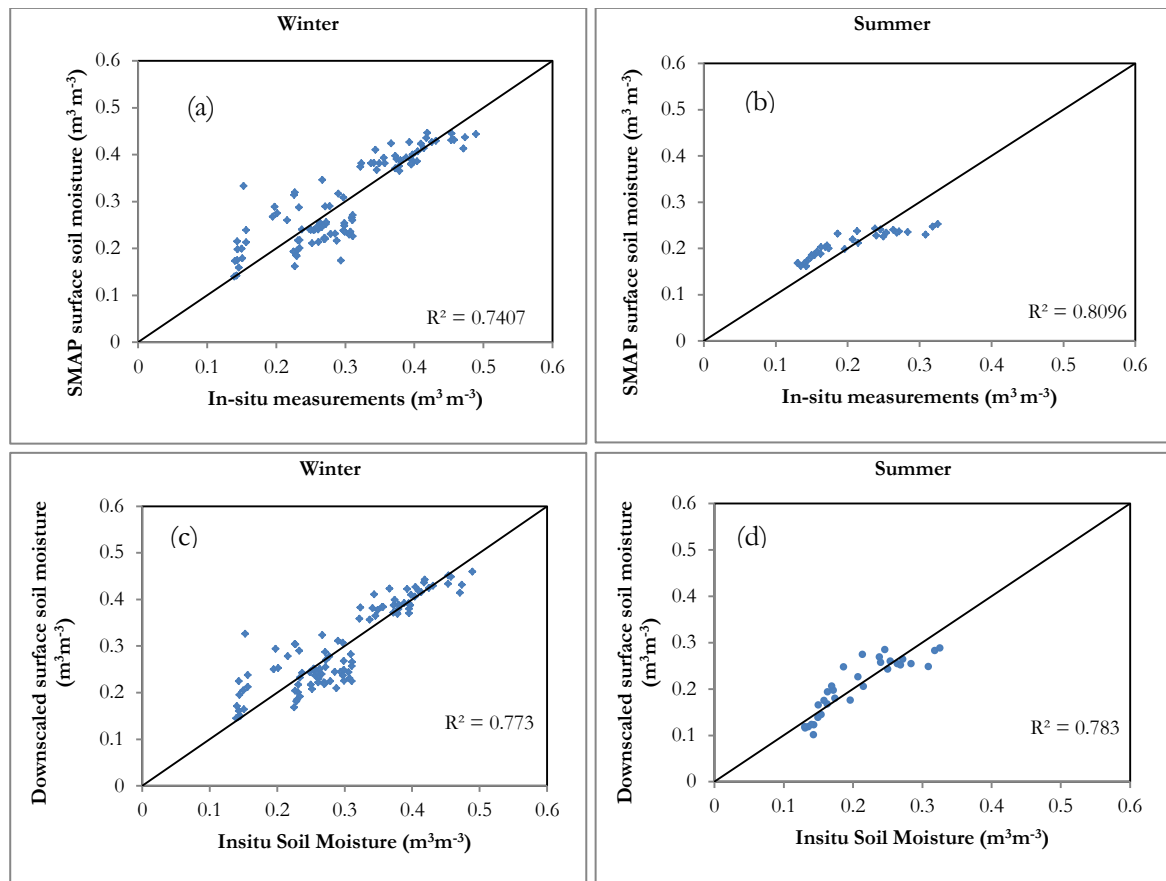


Figure 24: Scatter plot where (a) and (b) shows the agreements between SMAP surface soil moisture and in-situ measurements for summer and winter seasons and (c) and (d) shows the agreements between downscaled SMAP surface soil moisture and in-situ measurements.

9. FINAL REMARKS

9.1. Conclusions

Soil Moisture Active Passive Level 4 soil moisture (SMAP L4_SM) product which provides the global estimates for surface (5 cm depth) and root zone soil (1 m depth) moisture was used to analyse its applicability at a field scale through a downscaling approach using fine resolution Sentinel-1 SAR data. SMAP surface and root zone soil moisture indices were calculated from SMAP. Relationships between these surface and root zone soil moisture indices were developed for each pixel in the study area. These relationships were then used to calculate root zone soil moisture index from the downscaled surface soil moisture index at 50 m resolution. A baseline algorithm was used to downscale surface soil moisture index for which the soil sensitive parameters were obtained from the relationship developed between SMAP Level 4 surface soil moisture index and Sentinel-1 Synthetic Aperture Radar (SAR) backscatter from both VH and VV polarization. The downscaled surface and root zone soil moisture index were translated back to soil moisture content and were validated with the in-situ measurements. From the analysis and validation results it can be concluded that:

- A linear relationship was found between the SMAP surface soil moisture index and Sentinel-1 SAR backscatter, where in average the Sentinel-1 SAR backscatter increased by 1 dB for an increment of 0.1 in soil moisture index.
- The linear relationship between SMAP surface soil moisture and Sentinel-1 SAR backscatter is affected by the variation in incident angles. In this study the normalization of incidence angle was done using the Lambert's cosine law which improved the R^2 value from 0.313 to 0.418. Better relationships were obtained when the Sentinel-1 SAR data were separated according to their orbital passes (15, 37, 88 and 139) apparently being separated according different incidence angles and showed maximum R^2 value up to 0.644.
- The downscaled surface soil moisture for VH showed good correlation with the in-situ measurements but didn't matchup the accuracy of the original product whereas the downscaled soil moisture for VV showed a slight improvement in terms of unbiased root mean square error which increased from $0.066 \text{ m}^3 \text{ m}^{-3}$ to $0.062 \text{ m}^3 \text{ m}^{-3}$ and R^2 which increased from 0.573 to 0.593 when compared to original SMAP product.
- Although the downscaled surface soil moisture product did not meet the SMAP accuracy of $0.04 \text{ m}^3 \text{ m}^{-3}$ but was able to meet the accuracy requirement of high resolution soil moisture product ($0.06 \text{ m}^3 \text{ m}^{-3}$) and showed an improved result providing soil moisture data with much higher spatial resolution and land surface heterogeneity details. Thus, SMAP Level 4 surface soil moisture product can be quantified to the field scale for agricultural application through the downscaling approach proposed in this study.
- The accuracy assessment of estimated fine resolution root zone soil moisture showed degradation in terms of unbiased root mean square error and coefficient of determination value. The underlying catchment land surface model used for SMAP assimilation, which works in 9 km computational units, is not able to simulate the seasonal processes of the study area which resulted in the degradation of downscaled root zone soil moisture quality. The influencing factor in quantifying root zone soil moisture, like the presence of shallow groundwater table in the study area is not properly represented by the SMAP footprint which introduced errors in the downscaled root zone soil moisture product.
- The limitation in the validation process due to the scale mismatch of retrieved soil moisture with the point scale field measurement techniques still persists which can be considered as one of the reasons for less satisfying validation results in the case of root zone soil moisture because for root

zone soil moisture the number of stations available were limited when compared to surface soil moisture measurement stations.

9.2. Limitations and Recommendations

- The field measurements used for validation are point measurements whereas the SMAP L4_SM data are the average soil moisture data for every 9 square kilometres grid which limited our work of validation because of the scale mismatch. This limitation is recommended to look forward in future work.
- A further analysis is proposed on the soil moisture sensitive parameter, $\beta_{(C)}$ with respect to the temporal variability in surface heterogeneity (especially vegetation) is required one of which can be considering different $\beta_{(C)}$ values for different seasons (summer and winter) provided that a sufficient data for both the seasons are available. This analysis could not be done in this study because of the limited Sentinel-1 SAR data for summer period.
- The analysis of downscaled root zone soil moisture showed embedded imperfect parameterization in the model used for assimilation of SMAP Level 4 product, which hampered the result of downscaling and was a limitation of this research. So, a further check for conditions like shallow groundwater depth, seasonal variation is recommended.
- Application of downscaling approach for coarser resolution than 50 m is also recommended to evaluate the performance of baseline algorithm in presence of less speckle noise and to assess if the underlying model parameters and the performance of relationship developed between surface and root zone soil moisture becomes more representable in coarser resolution than 50 m.

LIST OF REFERENCES

- Ardila, J. P., Tolpekin, V., & Bijker, W. (2010). Angular backscatter variation in L-band ALOS ScanSAR images of tropical forest areas. *IEEE Geoscience and Remote Sensing Letters*, 7(4), 821–825. <https://doi.org/10.1109/LGRS.2010.2048411>
- Baldwin, D., Manfreda, S., Keller, K., & Smithwick, E. A. H. (2017). Predicting root zone soil moisture with soil properties and satellite near-surface moisture data across the conterminous United States. *Journal of Hydrology*, 546, 393–404. <https://doi.org/10.1016/j.jhydrol.2017.01.020>
- Bindlish, R., & Barros, A. P. (2001). Parameterization of vegetation backscatter in radar-based, soil moisture estimation. *Remote Sensing of Environment*, 76(1), 130–137. [https://doi.org/10.1016/S0034-4257\(00\)00200-5](https://doi.org/10.1016/S0034-4257(00)00200-5)
- Bousbih, S., Zribi, M., Lili-Chabaane, Z., Baghdadi, N., El Hajj, M., Gao, Q., & Mougenot, B. (2017). Potential of sentinel-1 radar data for the assessment of soil and cereal cover parameters. *Sensors (Switzerland)*, 17(11). <https://doi.org/10.3390/s17112617>
- Brocca, L., Hasenauer, S., Lacava, T., Melone, F., Moramarco, T., Wagner, W., ... Bittelli, M. (2011). Soil moisture estimation through ASCAT and AMSR-E sensors: An intercomparison and validation study across Europe. *Remote Sensing of Environment*, 115(12), 3390–3408. <https://doi.org/10.1016/j.rse.2011.08.003>
- Calvet, J. C., Wigneron, J. P., Walker, J., Karbou, F., Chanzy, A., & Albergel, C. (2011). Sensitivity of passive microwave observations to soil moisture and vegetation water content: L-band to W-band. *IEEE Transactions on Geoscience and Remote Sensing*, 49(4), 1190–1199. <https://doi.org/10.1109/TGRS.2010.2050488>
- Colliander, A., Jackson, T. J., Bindlish, R., Chan, S., Das, N., Kim, S. B., ... Yueh, S. (2017). Validation of SMAP surface soil moisture products with core validation sites. *Remote Sensing of Environment*, 191, 215–231. <https://doi.org/10.1016/j.rse.2017.01.021>
- Das, N. N., Entekhabi, D., & Njoku, E. G. (2011). An algorithm for merging SMAP radiometer and radar data for high-resolution soil-moisture retrieval. *IEEE Transactions on Geoscience and Remote Sensing*, 49(5), 1504–1512. <https://doi.org/10.1109/TGRS.2010.2089526>
- Das, N. N., Entekhabi, D., Njoku, E. G., Shi, J. J. C., Johnson, J. T., & Colliander, A. (2014). Tests of the SMAP combined radar and radiometer algorithm using airborne field campaign observations and simulated data. *IEEE Transactions on Geoscience and Remote Sensing*, 52(4), 2018–2028. <https://doi.org/10.1109/TGRS.2013.2257605>
- Das, N. N., Mohanty, B. P., Cosh, M. H., & Jackson, T. J. (2008). Modeling and assimilation of root zone soil moisture using remote sensing observations in Walnut Gulch Watershed during SMEX04. *Remote Sensing of Environment*, 112(2), 415–429. <https://doi.org/10.1016/j.rse.2006.10.027>
- Dataportal of the Dutch government. (2016). Basic registration Crop areas (BRP) - Datasets - Data.overheid.nl. Retrieved January 18, 2018, from <https://data.overheid.nl/data/dataset/basisregistratie-gewaspercelen-brp>
- Dente, L., Vekerdy, Z., Su, Z., & Ucer, M. (2011). *Twente soil moisture and soil temperature monitoring network*. Retrieved from https://www.itc.nl/library/papers_2011/scie/dente_twe.pdf
- Dumedah, G., Walker, J. P., & Merlin, O. (2015). Root-zone soil moisture estimation from assimilation of downscaled Soil Moisture and Ocean Salinity data. *Advances in Water Resources*, 84, 14–22. <https://doi.org/10.1016/j.advwatres.2015.07.021>
- English, N. B., Weltzin, J. F., Fravolini, A., Thomas, L., & Williams, D. G. (2005). The influence of soil texture and vegetation on soil moisture under rainout shelters in a semi-desert grassland. *Journal of Arid Environments*, 63(1), 324–343. <https://doi.org/10.1016/j.jaridenv.2005.03.013>

- Entekhabi, D., Njoku, E., O'Neill, P., Spencer, M., Jackson, T., Entin, J., ... Kellogg, K. (2008). The soil moisture active/passive mission (SMAP). In *International Geoscience and Remote Sensing Symposium (IGARSS)* (Vol. 3, p. III-1-III-4). IEEE. <https://doi.org/10.1109/IGARSS.2008.4779267>
- Entekhabi, D., Reichle, R. H., Koster, R. D., & Crow, W. T. (2010). Performance Metrics for Soil Moisture Retrievals and Application Requirements. *Journal of Hydrometeorology*, 11(3), 832–840. <https://doi.org/10.1175/2010JHM1223.1>
- Ferrazzoli, P., Paloscia, S., Pampaloni, P., Schiavon, G., Sigismondi, S., & Solimini, D. (1997). The potential of multifrequency polarimetric sar in assessing agricultural and arboreous biomass. *IEEE Transactions on Geoscience and Remote Sensing*, 35(1), 5–17. <https://doi.org/10.1109/36.551929>
- Giacomelli, A., Bacchiega, U., Troch, P. A., & Mancini, M. (1995). Evaluation of surface soil moisture distribution by means of SAR remote sensing techniques and conceptual hydrological modelling. *Journal of Hydrology*, 166(3–4), 445–459. [https://doi.org/10.1016/0022-1694\(94\)05100-C](https://doi.org/10.1016/0022-1694(94)05100-C)
- Houser, P. R., Shuttleworth, W. J., Famiglietti, J. S., Gupta, H. V., Syed, K. H., & Goodrich, D. C. (1998). Integration of soil moisture remote sensing and hydrologic modeling using data assimilation. *Water Resources Research*, 34(12), 3405–3420. <https://doi.org/10.1029/1998WR900001>
- Jackson, R. B., Canadell, J., Ehleringer, J. R., Mooney, H. A., Sala, O. E., & Schulze, E. D. (1996). A global analysis of root distributions for terrestrial biomes. *Oecologia*, 108(3), 389–411. <https://doi.org/10.1007/BF00333714>
- Kerr, Y. H., Waldteufel, P., Wigneron, J.-P., Delwart, S., Cabot, F., Boutin, J., ... Mecklenburg, S. (2010). The SMOS Mission: New Tool for Monitoring Key Elements of the Global Water Cycle. *Proceedings of the IEEE*, 98(5), 666–687. <https://doi.org/10.1109/JPROC.2010.2043032>
- Kim, Y., & van Zyl, J. J. (2009). A Time-Series Approach to Estimate Soil Moisture Using Polarimetric Radar Data. *Geoscience and Remote Sensing, IEEE Transactions on*, 47(8), 2519–2527. <https://doi.org/10.1109/TGRS.2009.2014944>
- Korres, W., Reichenau, T. G., & Schneider, K. (2013). Patterns and scaling properties of surface soil moisture in an agricultural landscape: An ecohydrological modeling study. *Journal of Hydrology*, 498, 89–102. <https://doi.org/10.1016/j.jhydrol.2013.05.050>
- Koster, R. D., Suarez, M. J., Ducharne, A., Stieglitz, M., & Kumar, P. (2000). A catchment-based approach to modeling land surface processes in a general circulation model 1. Model structure. *J. Geophys. Res.*, 105(D20), 24809–24822. <https://doi.org/10.1029/2000jd900327>
- Li, X., Chang, S. X., & Salifu, K. F. (2014). Soil texture and layering effects on water and salt dynamics in the presence of a water table: a review. *Environmental Reviews*, 22(1), 41–50. <https://doi.org/10.1139/er-2013-0035>
- Mladenova, I. E., Jackson, T. J., Bindlish, R., & Hensley, S. (2013). Incidence angle normalization of radar backscatter data. *IEEE Transactions on Geoscience and Remote Sensing*, 51(3), 1791–1804. <https://doi.org/10.1109/TGRS.2012.2205264>
- Mohanty, B. P., Cosh, M. H., Lakshmi, V., & Montzka, C. (2017). Soil Moisture Remote Sensing: State-of-the-Science. *Vadose Zone Journal*, 16(1), 0. <https://doi.org/10.2136/vzj2016.10.0105>
- Narayan, U., Lakshmi, V., & Jackson, T. J. (2006). High-resolution change estimation of soil moisture using L-band radiometer and radar observations made during the SMEX02 experiments. *IEEE Transactions on Geoscience and Remote Sensing*, 44(6), 1545–1554. <https://doi.org/10.1109/TGRS.2006.871199>
- NASA. (2014). SMAP Data Products. Retrieved August 6, 2017, from <https://smap.jpl.nasa.gov/data/>

- Njoku, E. G., & Entekhabi, D. (1996, October 1). Passive microwave remote sensing of soil moisture. *Journal of Hydrology*. Elsevier. [https://doi.org/10.1016/0022-1694\(95\)02970-2](https://doi.org/10.1016/0022-1694(95)02970-2)
- Njoku, E. G., Wilson, W. J., Yueh, S. H., Dinardo, S. J., Li, F. K., Jackson, T. J., ... Bolten, J. (2002). Observations of soil moisture using a passive and active low-frequency microwave airborne sensor during SGP99. *IEEE Transactions on Geoscience and Remote Sensing*, 40(12), 2659–2673. <https://doi.org/10.1109/TGRS.2002.807008>
- NSIDC. (2015). Data Fields - SMAP L4 Global 3-hourly 9 km Surface and Rootzone Soil Moisture. Retrieved August 22, 2017, from http://nsidc.org/data/docs/daac/smap/sp_l4_sm/data-fields.html
- Paloscia, S., Pettinato, S., Santi, E., Notarnicola, C., Pasolli, L., & Reppucci, A. (2013). Soil moisture mapping using Sentinel-1 images: Algorithm and preliminary validation. *Remote Sensing of Environment*, 134, 234–248. <https://doi.org/10.1016/j.rse.2013.02.027>
- Peng, J., Loew, A., Merlin, O., & Verhoest, N. E. C. (2017). A review of spatial downscaling of satellite remotely sensed soil moisture. *Reviews of Geophysics*, 55(2), 341–366. <https://doi.org/10.1002/2016RG000543>
- Peng, J., Loew, A., Zhang, S., & Wang, J. (2016). Spatial downscaling of global satellite soil moisture data using temperature vegetation dryness index. *IEEE Transactions on Geoscience and Remote Sensing*, 1(54), 558–566. <https://doi.org/10.1109/TGRS.2015.2462074>
- Pierdicca, N., Pulvirenti, L., Bignami, C., & Ticconi, F. (2013). Monitoring soil moisture in an agricultural test site using SAR data: Design and test of a pre-operational procedure. *IEEE Journal of Selected Topics in Applied Earth Observations and Remote Sensing*, 6(3), 1199–1210. <https://doi.org/10.1109/JSTARS.2012.2237162>
- Piles, M., Entekhabi, D., & Camps, A. (2009). A change detection algorithm for retrieving high-resolution soil moisture from SMAP radar and radiometer observations. *IEEE Transactions on Geoscience and Remote Sensing*, 47(12), 4125–4131. <https://doi.org/10.1109/TGRS.2009.2022088>
- Pitts, L. (2016). Monitoring Soil Moisture for Optimal Crop Growth – Help Desk. Retrieved August 17, 2017, from <https://observant.zendesk.com/hc/en-us/articles/208067926-Monitoring-Soil-Moisture-for-Optimal-Crop-Growth>
- Reichle, R., De Lannoy, G., Liu, Q., Ardizzone, J., Kimball, J., & Koster, R. (2016). SMAP Level 4 Surface and Root Zone Soil Moisture. In *International Geoscience and Remote Sensing Symposium (IGARSS)* (Vol. 2016–Novem, pp. 136–138). IEEE. <https://doi.org/10.1109/IGARSS.2016.7729026>
- Sánchez, N., González-Zamora, Á., Piles, M., & Martínez-Fernández, J. (2016). A new Soil Moisture Agricultural Drought Index (SMADI) integrating MODIS and SMOS products: A case of study over the Iberian Peninsula. *Remote Sensing*, 8(4). <https://doi.org/10.3390/rs8040287>
- Schneider, S., Jann, A., & Schellander-Gorgas, T. (2014). Downscaling of seasonal soil moisture forecasts using satellite data. *Hydrology and Earth System Sciences*, 18(8), 2899–2905. <https://doi.org/10.5194/hess-18-2899-2014>
- Sentinel 1 Team. (2013). ESA Sentinel 1 handbook. <https://doi.org/10.1017/CBO9781107415324.004>
- SMAP Science Team. (2014). *SMAP Handbook. Mapping Soil Moisture and Freezes/Thaw from Space*.
- Song, C., Jia, L., & Menenti, M. (2014). Retrieving high-resolution surface soil moisture by downscaling AMSR-E brightness temperature using MODIS LST and NDVI data. *IEEE Journal of Selected Topics in Applied Earth Observations and Remote Sensing*, 7(3), 935–942. <https://doi.org/10.1109/JSTARS.2013.2272053>
- Taktikou, E., Bourazanis, G., Papaioannou, G., & Kerkides, P. (2016). Prediction of Soil Moisture from

Remote Sensing Data. In *Procedia Engineering* (Vol. 162, pp. 309–316). <https://doi.org/10.1016/j.proeng.2016.11.066>

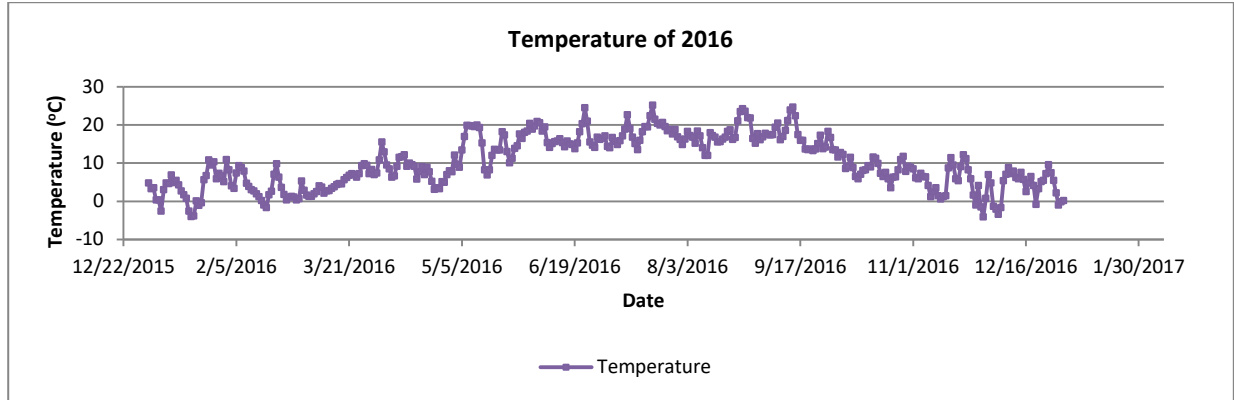
van der Velde, R., Salama, M. S., Eweys, O. A., Wen, J., Wang, Q., Velde, R. Van Der, ... Wang, Q. (2014). Soil Moisture Mapping Using Combined Active / Passive Microwave Observations Over the East of the Netherlands. *IEEE Journal of Selected Topics in Applied Earth Observation and Remotesensing*, 8(9), 1–18. <https://doi.org/10.1109/JSTARS.2014.2353692>

Yue, J., Yang, G., Qi, X., & Wang, Y. (2016). Soil moisture retrieval in well covered farmland by radarsat - 2 sar data. *2016 IEEE International Geoscience and Remote Sensing Symposium (IGARSS)*, (3), 1699–1702. <https://doi.org/10.1109/IGARSS.2016.7729434>

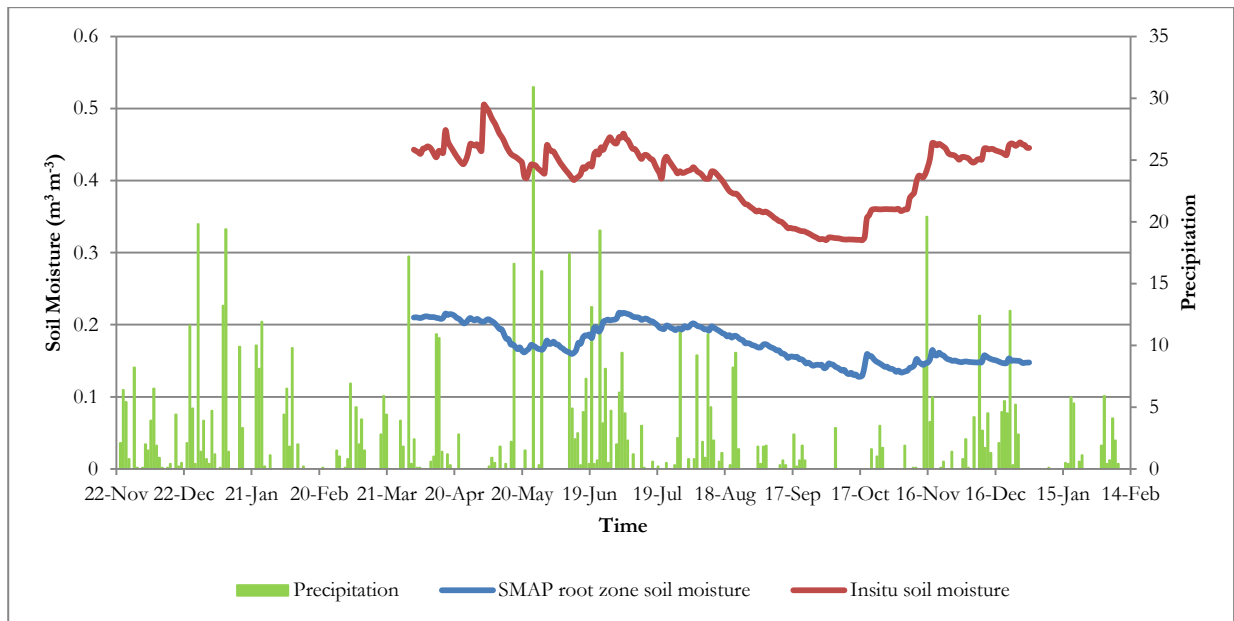
Zhang, X., Zhang, T., Zhou, P., Shao, Y., & Gao, S. (2017). Validation analysis of SMAP and AMSR2 soil moisture products over the United States using ground-based measurements. *Remote Sensing*, 9(2), 104. <https://doi.org/10.3390/rs9020104>

APPENDICES

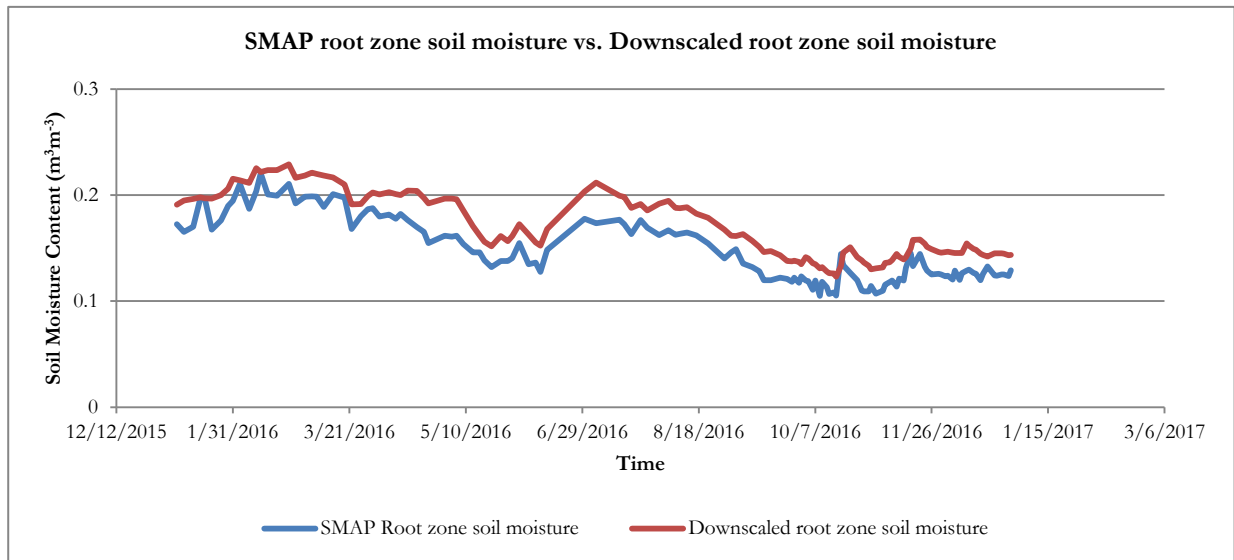
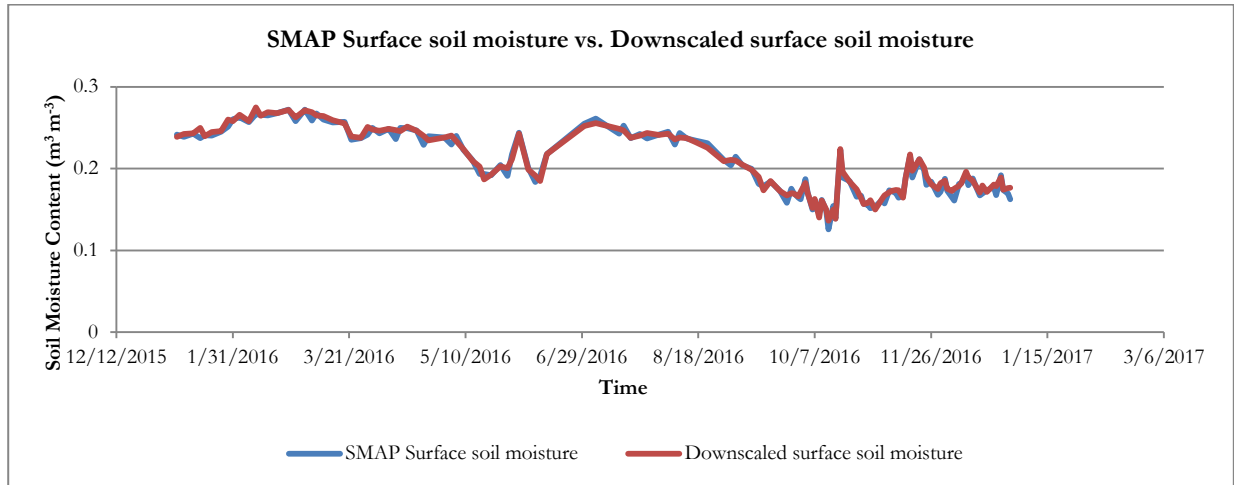
Appendix 1: Dynamics of temperature in Twente region for the year 2016 obtained from KNMI.



Appendix 2: Time series showing the averaged retrieved coarse resolution SMAP root zone soil moisture against the averaged in-situ soil moisture measurements (weighted averages of 80 cm soil surface) and the rainfall data.



Appendix 3: Time series of SMAP surface soil moisture with Downscaled surface soil moisture and SMAP root zone soil moisture with Downscaled root zone soil moisture.



Appendix 4: Scatter plot showing the agreements between SMAP root zone soil moisture and in-situ measurements and between downscaled root zone soil moisture and in-situ measurements separated for summer and winter seasons.

